



**KAUNAS UNIVERSITY OF TECHNOLOGY
FACULTY OF MECHANICAL ENGINEERING AND DESIGN**

Gobinath Siva

**DEVELOPMENT OF FINITE ELEMENT MODEL FOR NEW TYPE
PIEZOELECTRIC COMPOSITE MATERIAL**

Master's Degree Final Project

Supervisor

Assoc Prof. Dr. Giedrius Janusas

KAUNAS, 2017

KAUNAS UNIVERSITY OF TECHNOLOGY
FACULTY OF MECHANICAL ENGINEERING AND DESIGN

**DEVELOPMENT OF FINITE ELEMENT MODEL FOR NEW TYPE
PIEZOELECTRIC COMPOSITE MATERIAL**

Master's Degree Final Project
Industrial Engineering and Management (621H77003)

Supervisor

(signature) Assoc. prof. Dr. Giedrius Janusas
(date)

Reviewer

(signature) Lecturer. Dr. Rokas Sakalys
(date)

Project made by

(signature) Gobinath Siva
(date)

KAUNAS, 2017



KAUNAS UNIVERSITY OF TECHNOLOGY

Faculty of Mechanical Engineering and Design

Gobinath Siva

Industrial Engineering and Management 621H77003

DEVELOPMENT OF FINITE ELEMENT MODEL FOR NEW TYPE PIEZOELECTRIC
COMPOSITE MATERIAL

DECLARATION OF ACADEMIC INTEGRITY

_____ 20 _____
Kaunas

I confirm that the final project of mine, **Gobinath Siva**, on the subject “Development of finite element model for new type piezoelectric composite material” is written completely by myself; all the provided data and research results are correct and have been obtained honestly. None of the parts of this thesis have been plagiarized from any printed, Internet-based or otherwise recorded sources. All direct and indirect quotations from external resources are indicated in the list of references. No monetary funds (unless required by law) have been paid to anyone for any contribution to this thesis.

I fully and completely understand that any discovery of any manifestations/case/facts of dishonesty inevitably results in me incurring a penalty according to the procedure(s) effective at Kaunas University of Technology.

(name and surname filled in by hand)

(signature)

**KAUNAS UNIVERSITY OF TECHNOLOGY
FACULTY OF MECHANICAL ENGINEERING AND DESIGN**

Approved:

Head of
Production engineering
Department

(Signature, date)

Kazimieras Juzėnas

(Name, Surname)

**MASTER STUDIES FINAL PROJECT TASK ASSIGNMENT
Study programme INDUSTRIAL ENGINEERING AND MANAGEMENT**

The final project of Master studies to gain the master qualification degree, is research or applied type project, for completion and defence of which 30 credits are assigned. The final project of the student must demonstrate the deepened and enlarged knowledge acquired in the main studies, also gained skills to formulate and solve an actual problem having limited and (or) contradictory information, independently conduct scientific or applied analysis and properly interpret data. By completing and defending the final project Master studies student must demonstrate the creativity, ability to apply fundamental knowledge, understanding of social and commercial environment, Legal Acts and financial possibilities, show the information search skills, ability to carry out the qualified analysis, use numerical methods, applied software, common information technologies and correct language, ability to formulate proper conclusions.

1. Title of the Project

DEVELOPMENT OF FINITE ELEMENT MODEL FOR NEW TYPE PIEZOELECTRIC COMPOSITE MATERIAL

Approved by the Dean Order No. V25-11-8, 21 April 2017

2. Aim of the project

To develop the finite element model for the piezoelectric composite material and comparing the results of theoretical and experimental calculations.

3. Structure of the project

1. Literature Review
2. Experimental setup
3. Theoretical Calculations
4. Finite Element model and simulations

4. Requirements and conditions

No specific requirements

5. This task assignment is an integral part of the final project

6. Project submission deadline: 2017 MAY 31

Student

Gobinath Siva

(Name, Surname of the Student)

Supervisor

Assoc Prof. Dr. Giedrius Janusas

(Position, Name, Surname)

(Signature, date)

(Signature, date)

Gobinath Siva. Development of finite element model for new type piezoelectric composite material. Master's Final Project in industrial engineering and management. Supervisor Assoc. prof. Dr. Giedrius Janusas, Faculty of Mechanical Engineering and Design, Kaunas University of Technology.

Research field and area: Technological science, production engineering

Keywords: Microcantilever, Mechanical vibration.

Kaunas, 2017. 41 p.

SUMMARY

The project involves the development of finite element model for a piezoelectric material. The material used in this research work is PZT (Lead Zirconate Titanate) which is a widely used PZT Ceramic material because of its lower cost and versatility design. Different fabrication method has been carried out for the construction of the PZT element. A screen-printing technique was used for the preparation of specimen to apply a smooth and equal thickness of the formed thin films of thickness 1. 2 μ m. An electrical pole alignment technique was applied to improve the voltage characteristics of the PZT element. Theoretical and experimental calculations were made using Finite element method. The results of from the simulations were compared with the results from theoretical and experimental calculations.

Gobinath siva. Naujo tipo pjezoelektrinio kompozito baigtinių elementų modelio kūrimas. Pramonės inžinerijos ir vadybos magistro baigiamasis projektas vadovas Assoc. prof. Dr. Giedrius Janusas. Kauno technologijos universitetas, Mechanikos inžinerijos ir dizaino fakultetas.

Mokslo kryptis ir sritis: Technologiniai mokslai, gamybos inžinerija

Reikšminiai žodžiai: mikrokonsolė, mechaninė vibracija.

Kaunas, 2017 m. 41 p.

SANTRAUKA

Projekto metu kuriamas baigtinių elementų modelis pjezoelektrinei medžiagai. Tiriamajame darbe naudojama ŠCT (švino cirkonato titanatas) medžiaga. Ši medžiaga plačiai naudojama keramikos srityje, nes jos kaštai maži, o dizainas įvairiausias. ŠCT elemento sudarymui naudotasi skirtingais gamybos metodais. Mėginių paruošimui panaudota momentinės ekrano kopijos technologija, dėl ko susidariusios 1,2 μm storio plėvelės buvo glotnios ir vienodo storio. ŠCT elemento įtampos charakteristikoms pagerinti naudota elektrinių polių sulyginimo metodas. Teoriniai ir eksperimentiniai skaičiavimai atlikti, naudojant baigtinių elementų metodą. Imitavimo metu gauti rezultatai palyginti su teorinių ir eksperimentinių apskaičiavimų rezultatais.

ACKNOWLEDGEMENT

I take it as a privilege to express my profuse thanks to my beloved advisor and reviewer lecturer Assoc. prof. Dr. Giedrius Janusas of Mechanical Engineering department in Faculty of Mechanical Engineering and Design, for his kind guidelines and support which allow me for completing the final semester project.

CONTENTS

LIST OF FIGURES	8
INTRODUCTION	9
1. LITERATURE REVIEW	10
1.1 MICRO RESONATORS	10
1.2. PZT MATERIALS	10
1.2.1 Types of Piezoelectric Materials:	10
1.2.2 Why PZT?	11
1.2.3 Manufacturing Process:	13
1.2.4 Typical PZT Characteristics:	14
1.2.5 Applications:	14
1.3 FINITE ELEMENT METHOD OF COMPOSITE MATERIALS	15
2. EXPERIMENTAL SETUP	20
2.1 SPECIMEN PREPARATION	21
2.1.1 PZT Composite Fabrication	21
2.2 PROCESS OF MAKING THE ELEMENT	22
2.2.1 Screen printing technique	22
2.3 ELECTRICAL POLE ALIGNMENT	23
2.4 Prism System	Error! Bookmark not defined.
3.THEORETICAL CALCULATION	25
3.1 THEORETICAL CALCULATION WITH FORMULA	25
3.2 COMSOL Multiphysics	29
3.3 Comparison of Theoretical and Experimental Results	31
4.Results	33
5.CONCLUSIONS	35
References	Error! Bookmark not defined.

LIST OF FIGURES

Figure 1-1 Crystal structure of the lead zirconate titanate (PZT).....	12
Figure 1-2 The Process of Manufacturing PZT	13
Figure 2-1 Experimental Setup.....	20
Figure 2-2 Plan of Piezoelectric Element	22
Figure 2-3 Model of rectangular cantilever beam	29
Figure 2-4 Pole Alignment Setup	23
Figure 2-5 Pole Alignment Setup	24
Figure 3-1 Mode shapes of cantilever beam.....	28
Figure 3-2 Modelling of PZT Composite material using COMSOL Multiphysics.....	31
Figure 4-1 Frequency analysis.....	33
Figure 4-2 Vibrational analysis	34

INTRODUCTION

Piezoelectricity is no modern discovery. When the Curies discovered the property in the late 19th century, they might not have imagined that their discovery would become one of the most sought of research in the 20th century. The property to generate electricity when a mechanical stress is given and the reverse nature to create mechanical work when electricity is given is a phenomenon naturally occurring in the Quartz crystal. With the advancement in the fields of Science and Technology, artificial materials such as Lead Zirconate Titanate were produced to harness energy and work. One could say that the areas of application of the piezoelectric material are vast and the potential to study them, apply them and use them grows day by day with further studies around the globe.

The artificially made Piezoelectric elements come incorporating different forms the Piezoelectric material. The most common are Lead Zirconate Titanate ceramic powder coating as a composite and the Polymer-based PVDFs. The naturally occurring Quartz is also used but on a very small scale and not for these electrical, electronic and mechanical elements as it would be highly expensive.

This research is about creating PZT ceramic material with different compositions and using them to create cantilever beam element which would be used to study the modes of the frequency of vibrations of the beam. The research work also covers analyzing the created PZT cantilever element connected with a micro-resonator and a Finite element analysis of the beam using COMSOL Multiphysics. Using COMSOL Multiphysics for Finite Element Analysis of the PZT element significantly gives a better approach to studying the created PZT material and the Cantilever element. Other programs such as MATLAB have also been used but only for theoretical calculation purposes.

AIM

To develop Finite Element Model for a new type Piezoelectric Composite material.

Tasks

To do an experimental analysis of the prepared PZT composite samples.

To calculate theoretical eigenfrequencies and eigenmodes of the created samples.

Using theoretical and experimental results to create FE model of PZT composite material.

1. LITERATURE REVIEW

1.1 MICRORESONATORS

Micro resonators are micrometer-scale structures for confining light. Light is reflected internally at the edges of the resonator. This creates a series of standing-wave optical modes, or resonances, like those that can exist on a vibrating guitar string. Microresonators have the ability to provide the optical feedback needed for the working of semiconductor lasers.

For experimentations, three measurements are taken into account namely *gain, the sharpness of peak, and the quality-factor* (Lerman & Elata, 2010, pp. 1-3). These are usually measured mathematically by Log Decrement method. Lerman & Elata further explain making distinctions of single and double port eletromechanical resonators and also provide informations as to why anti-resonance occurs. They also make analysis on the distribution systems. The product of frequency and quality factor ($f \cdot Q$) in distributed systems should be re-calculated. A microresonator design has many potential reasons of which Lerman & Elata state one of them. One of the main aim in designing any microresonator is to achieve *high quality factors at high frequencies* (Lerman & Elata, 2010). It gives one of the main reasons to know and *to understand what affects common measures of quality-factor* (Lerman & Elata, 2010) and in what way these measured values are affected and change in a given system. However, it is very difficult to measure these practically. It could be said that these estimated values of quality-factor can be accurate in case of any linear resonator driven mechanically with a single degree of freedom. In general, it is believed that at any given resonance frequency, the value calculated as a product of frequency and quality factor is always a constant.

1.2. PZT MATERIALS

Piezoelectric materials are those materials exhibiting the piezoelectric property which is creating electricity due to application of a mechanical stress. They also work the other way around.

1.2.1 Types of Piezoelectric Materials:

The Piezoelectric materials are either naturally occurring or artificially made. Some of the naturally occurring piezoelectric crystals are *quartz ($Si O_2$), Rochelle salt, Topaz, Tourmaline-group minerals and some organic substances as silk, wood, enamel, dentin, bone, hair, rubber.* (Dineva, Gross, Muller, & Rangelov, 2014)

The artificially made piezoelectric materials are piezo-ceramics, chemical-polymers, and composites.

The following are some of artificially made ceramics,

perovskite: Barium titanate ($BaTiO_3$)

Lead titanate ($PbTiO_3$)

Lead zirconate titanate ($Pb[Zr_xTi_{1-x}]O_3$, $0 < x < 1$) - commonly referred to as PZT

Potassium niobate ($KNbO_3$)

Lithium niobate ($LiNbO_3$)

Lithium tantalate ($LiTaO_3$), etc. and other lead-free piezoceramics.

1.2.2 Why PZT?

PZT is the most commonly used ceramic material. It is commercially available in the market in different sizes and configurations. The *high piezoelectric coupling coefficients and relatively low maximum operating temperature (200°C)* (Mohammadi, 2013) are some of the great advantages of using PZT ceramics. There are also other advantages over naturally occurring quartz such as *lower cost and versatility in design* (Mohammadi, 2013) by altering the mixture composition and their characteristic properties.

It should be noted that these PZT ceramics also have higher piezoelectric charge sensitivity in them but on the other hand, there are also few disadvantages like *lower stability, loss of polarization, aging, and fatigue* (Mohammadi, 2013). However, *many materials exhibit the piezoelectric effect to a much lesser degree* (Joe, 2009). In comparison with other materials, Ceramics (PZT) offers, good span, passive, accurate, good resolution, linear, cheap, and easy to find and work with.

Among the whole family of artificial piezoelectric materials, PZT has been mostly associated with making transducers. *This family of ceramics has high values for the piezoelectric charge coefficient, electromechanical coupling coefficient, and dielectric constant* (T & S) and also lower electrical losses.

PZT, as a perovskite crystal structure has *a small tetravalent metal ion in a lattice of large divalent metal ions* (APC International, 2016), wherein the former is usually a Titanium and a Zirconium and the latter is Lead.

In general, piezoelectric materials like PZT exhibit a unique range of properties. In simple words, when a piezoelectric material is subjected to deformation, an electric charge is generated at an angle perpendicular to the direction of application of mechanical load. This is known as the piezoelectric effect. The other way around of this is known to be the reverse or inverse piezoelectric effect. It is when

an electric field is applied to a piezoelectric material, deformation occurs at an angle perpendicular to the direction of applied of electric field.

In the last decade, these piezoelectric materials have considerably attracted interests among researchers for several reasons. In particular, the PZT class of materials have been the focus for some time among researchers because of its simple basic crystal structure. Unlike other crystalline structures, absence of closely packed oxygen framework is an added advantage. This eases the flexibility for any chemical substitution. It also provides easy altering of physical properties as per the requirement.

When compared with the *previously discovered metallic oxide based piezoelectric material Barium Titanate*, PZT materials exhibit greater sensitivity and have a higher operating temperature. (APC International, 2016). PZT, has dominated the market because of its superior dielectric and piezoelectric nature.

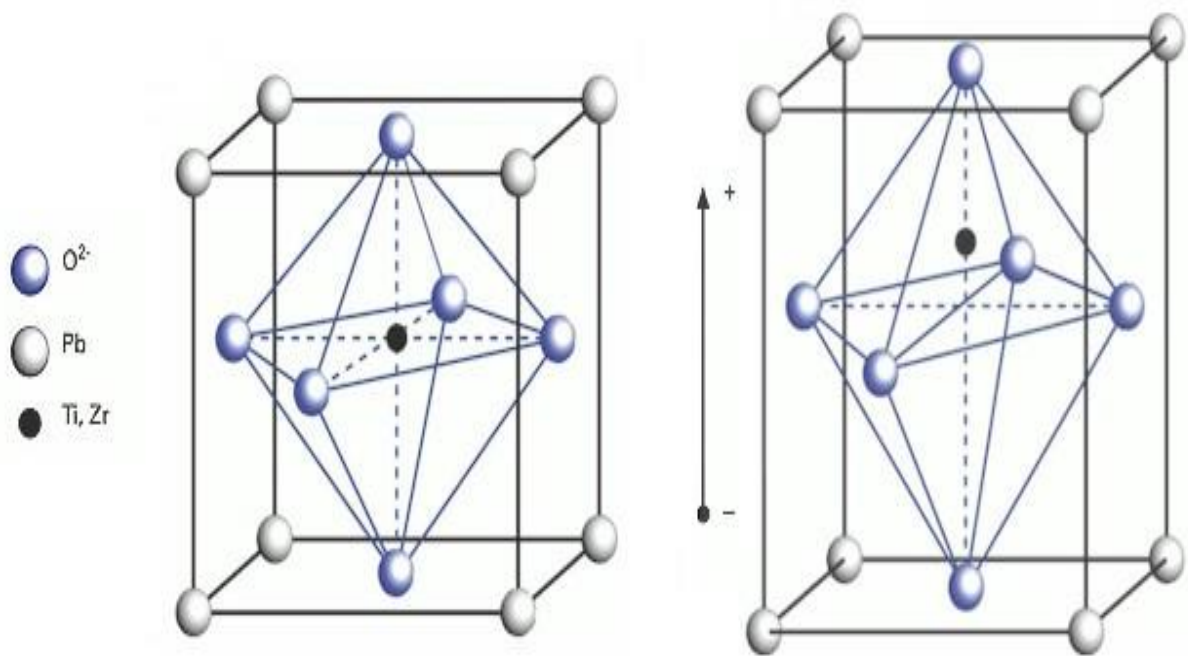


Figure 1-1 Crystal structure of the lead zirconate titanate (PZT) [Source - APC International, 2016]

1.2.3 Manufacturing Process:



Figure 1-2 The Process of Manufacturing PZT [Source - APC International, 2016]

The process associated with the manufacturing of PZT powders involves six separate processes. Raw materials with higher purity and material activity are studied and sourced around the globe.

The instant they are sourced and approved for manufacturing process, they are weighed and transferred to wet mills. Initially, these raw materials are wet-milled together at suitable proportions to achieve a uniform particle size distribution. There has to be proper control over particle size distribution because that is needed to ensure uniform material activity during the process of calcination.

After the wet milling process, the product is heat dried and prepared for the process of calcining. *The product must be calcined in high-purity crucibles to guarantee no chemical contaminants are present in the final product* (APC International, 2016). The calcining process takes place at a temperature of about 1000°C, during which the required PZT phase is formed.

It is important to remember that the major ingredient in PZT material is the lead oxide, which is a hazardous material with a relatively high vapor pressure at calcining temperatures (APC International, 2016). Proper measures are taken to ensure that lead loss is not a factor accounted for.

After the process of calcining, the PZT powder is brought back to the wet-mill. This is done to employ homogeneity and to have the material ready for further addition of an organic binding agent. After this stage, the slurry led to a spray dryer. Here the moisture is evaporated. After a successful spray drying operation which involves experienced operators regulating the temperatures and the quantity of slurry entering the spray drying unit.

The whole purpose of this drying process is to provide a free-flowing product. This in turn ensures to consistently fill cavities when manufacturing piezoelectric ceramics. With the uniform nature of PZT spheres' particle size distribution, it *allow for air escapement throughout the compaction process, yielding lamination-free green ceramic shapes.* (APC International, 2016)

1.2.4 Typical PZT Characteristics:

- High output.
- High frequency with fast response time.
- Higher sensitivity
- Compatible with low and high voltage drive circuits.
- High amount of mechanical and acoustic coupling.
- Different customized shapes and sizes as per need.
- Different compositions as per need.

1.2.5 Applications:

If required, for virtually any application, piezoelectric system can be developed. Although, the size, weight and price of the piezoelectric elements are some of the limiting factors when one considers to use them in any applications. There are four different ways using Piezo ceramic materials which are as follows,

- ✓ Piezo Generators
- ✓ Sensors
- ✓ Piezo Actuators
- ✓ Transducers

Common application areas (CeramTec, 2017) are

- Sea-bed and Ocean depth exploration (sonar, beacons).
- Aeronautical and Aerospace Engineering (gyroscopes, accelerometers, level sensing).
- Medical Engineering products such as Doppler blood flow, dental descaling, general surgery, bubble detection, etc.
- Consumer-end products like ultrasonic toothbrushes, jewellery cleaners, contact lens cleaners, computer hard drives, touch screen displays, etc.

- Industrial and Commercial items like flow and level sensors, ultrasonic cleaning, ultrasonic welding, intrusion alarms, fabric needle positioning, machine vibration monitoring, bubble detection, sonochemistry, etc.
- Telecommunication instrumentation and engineering (optical switching of telecom lines, buzzers, and alarms, Haptics feedback, mobile phone cameras).
- *Automotive (power seat controls, reversing/collision avoidance sensors, anti-knock sensors).*
- *Scientific research (Nano positioning stages and analytical tools, scanning probe microscopy, advanced acoustics).*

1.3 FINITE ELEMENT METHOD OF COMPOSITE MATERIALS

Composite laminated materials are actively used *due to their long fatigue life, high stiffness, high strength to weight ratio, resistance to electrochemical corrosion and many more other material properties.* (Wangikar, Jadhav, & Patil, 2014). They say “*a proper understanding of their structural behavior is required*”. Finite element method, herein after referred to as FEM, is in particular very versatile and efficient to use in analyzing the complex structural behavior. FEM has been closely associated with a large number of research *devoted to the analysis of de-lamination, vibration, dynamics, buckling, post-buckling failure and damage analysis.* (Wangikar, Jadhav, & Patil, 2014)

Composite laminates are layers of fibrous composite materials. They portray engineering properties such as in-plane stiffness, bending stiffness, etc. When plywood is used, the composite laminate is referred to as a hybrid composite. The mechanical properties are known by its configuration, including fiber volume fraction and in-plane fiber distribution. The various mechanical properties of a composite material depend on:

- Properties of incorporating materials.
- Orientation of layers.
- Volume fractions of each element of the composition.
- Thickness of layers.
- Bonding nature between layers.

With the increasing interest in the modern composites applications in the field of engineering, there has also been an increasing need to improve the numerical modelling techniques for such materials.

Previously, thermal loading of FGM coatings has been modelled by series expansion-based methods as well as finite element and boundary element methods. In line with the application of known algorithms, new approaches are developed with the aim of improving the accuracy and flexibility of modelling. (K & T, 2009). Among other methods, mesh-free or meshless schemes, competing with the standard finite element method, are novel numerical techniques that find continuously growing application fields in material science and engineering. K. Nakonieczny, and T. Sadowski discussed modelling Composite materials for Thermal shocks using Mesh less Finite Element Method.

Accuracy in modeling composite shells is governed by the first-order shear-deformation theory (commonly referred to as Mindlin-Reissner shell theory) (SAS IP, 2017) As for as the modelling is concerned, the properties of the material were first incorporated into Autodesk composite analysis software. The macro given, is used to import the material properties into Ansys. In context with the boundary conditions, with the bottom plate being the fixed end and with restricted DOF, a constant displacement of 0.06in is provided to imitate the tensile testing environment. (E & E.L, 2014)

In order to model multilayer sheet, the procedure is repeated for each layer to obtain the whole material. The algorithm describes this approach. Indeed, the duplication of nodes and edges of the thin region is done as many times as the number of sheets. It can be seen that the results obtained by the finite element model and the shell element model are close. An error of 3.9% between the two models is observed. However, the number of elements is divided by three. This shows the value of using multilayer shell elements. B. Ramdane et al have discussed in detail about the Electromagnetic and Thermal modelling of Composite materials using Multi-layer shell elements and was able to conclude that the FEM model and Shell model showed similar results.

For modelling, another approach such as Multi-continuum method can also be adapted. The whole concept of the multi-continuum mechanics was proposed by Garnich and Hansen. The concept on which their proposal was based on the ideology of composite to constituent stress and strain decomposition which was told by Hill previously. The initially suggested idea for analysis of failures by Garnich and Hansen was used by Mayes and Hansen in the later period. It was then they created an improved version of von Mises failure criteria. This further provided with better solutions. *The multi continuum method is practically best suited for composite analysis which gives complete insight about the fiber failure in all the layers of the material* (E & E.L, 2014). This method makes the simulation of composite easy and economical which ultimately gets the best products in the market for the improvement of humans.

The modelling of the fatigue behavior of composite material during three-point bending tests have been proposed by various works. These are based on the fatigue modulus reduction of laminate composites and of the sandwich composites. The fatigue modulus which is generally referred as stiffness can be defined as being the ratio between the applied stress and the strain at a given number of cycles.

Fatigue tests were performed using displacement control with applied sinusoidal waveform of constant static mean displacement d_{mean} and amplitude d_{am} . During the tests, the decrease in load (stiffness) according to the number of cycles was recorded. Fatigue tests were performed using load control. The applied waveform is sinusoidal with a constant static mean load F_{mean} and amplitude F_{am} . During the tests, increase in displacement according to the number of cycles was recorded. A. El Mahi et al have thus discussed the modelling of sandwich panels.

- LINK8 component is a one-dimensional box component having strain and pressure properties just, which implies that no twisting tension is considered. The component contains six DOF: each of the two knob of the component can turn in x, y and z-path. Component definition passes by its area of the two knobs, the cross segment, and the doled out material properties.
- SHELL63 component is two-dimensional, three knob (triangular) or four-knob component with twisting and film abilities. Every hub has six DOF: interpretation in x, y and z-path and turn around the x, y and z-hub. Component definition passes by the area of the hubs, the thickness, and the comparing material properties.
- SOLID45 component is a six (triangular) or eight (rectangular) hub component with three DOF in every hub: along x, y and z-knob. Component definition passes by the area of the eight hubs and the relating material properties.

While in the replacement approach layer one always has the first material property and layer two the other, this distribution varies dependent on the direction of the stress. This leads to the truth that and tensile and compressive stresses are interchanged on one direction. With low minor thickness of the material and a uniform material behavior, the resulting error is negligible. Results confirm that the plane fiber approach is not suitable to validate the simulation of the fiber reinforced composite material. Therefore, the woven approach seems to be the choice to be used for obtaining the average material numbers for the approach for three-dimensional structures.

A Domain Superposition Technique (DST) is made for the simulation of woven fabric composites. Without explicit modelling of the tows and the likely degeneration resin pocket regions among tows, DST develops the tow region and the matrix region. They are both non-degenerate. They can be easily discretized using the traditional solid elements. An improved version of the material model is used for tow elements. Material properties of elements in the same space are subtracted from each other. If the initial tow elements have properties assigned as tow minus matrix, then when the matrix properties are

added, only the tow properties remain. The two regions are then superimposed by coupling them together. When compared to commonly used mesh superposition methods that usually involve with high iterative procedures, using DST method is very easy and simple. The study was done on three different meshes of the Layer-to-Layer weave style. PG Biragoni and SR Hallett make a detailed discussion on the FEM modelling of 3D woven composites for Stiffness Prediction.

If one wishes to use COMSOL, to create meshes of the laminate element, QUAD is used. The size of each element is chosen as $25 \mu\text{m} \times 25 \mu\text{m}$ with the minimum element quality value at 0.99 and the minimum element area ratio at 0.96. Two-dimensional modelling involves considering the plane strain. Time-dependent analysis along with Lagrangian quadratic type of element were used for solving FEM. UMFPAK is used for obtaining the solution on that regard. The duration for the solution was to be 200 μs wherein the complete signal is captured. The time steps used is 100 ns. BDF scheme of order 2 as an integration technique was used. Bikash Ghose et al successfully developed a FEM model of composites using COMSOL.

For studying of the free edge effect associated with the inter-laminar stress caused shear, most works previously done focused on the uniform axial loads. This loading condition does not create any new stress components like out-of-plane stresses, which however has no important effect on the bending of the PZT element and its failure behavior. In addition to that, with the decrease of the support span, these stress components associate with a growing vital role in the composite failure modes. The reasons can be such as the nature of bending which is subjected to the laminate tension, compression, and shear. Therefore six stress components should be considered while calculating the criteria for fail.

COMSOL Multiphysics package adapted FEM and was used to evaluate the performance of a composite piezoelectric beam. For both cases, the simulation results have shown some light on the fact that PM32 has the highest greatest voltage generation ability which was followed by PZT-5A in the second place. PZT-4 in was ranked third while PZT-5H came fourth with the lowest value of electric potential. Not only having large values of electrical potential, the model using PMN32 also results in values with the highest average of the electric field, electric energy density, etc. On the other hand, PMN32 material model has the lowest first resonance frequency of compared to the PZT models. As for the possible future studies, the strong piezoelectric effect shown by PMN32 needs to be explored, particularly in regards with the vibration to electric power generation. This enables material properties optimizations and design geometry of the cantilever device.

These components assume a vital part in shaping the dielectric and piezoelectric reaction and the variable piezoelectric anisotropy of the permeable media in the wide porosity and polymer extend. It is seen that both piezoelectric affectability and anisotropy of the absorptive ceramics and composites are nearly anticipated as far as the fixation parameters. In addition, as takes after from correlation of the test and computed comes about, the upper bound 0.60 is a reasonable gauge where the proposed model is dependable for microstructural design and enhancement of permeable piezo-dynamic materials for specific applications.

2. EXPERIMENTAL SETUP

The dynamic investigations consist of an experimental setup with a Piezoelectric Energy Harvester (PVEH) that applies single hits, excitation, measurement systems and data acquisition. The Data Acquisition System consists of the following,

- 4 Channel USB Oscilloscope (Analog to Digital Converter)
- PicoScope 6000 Series (as shown in the photoshoot below)

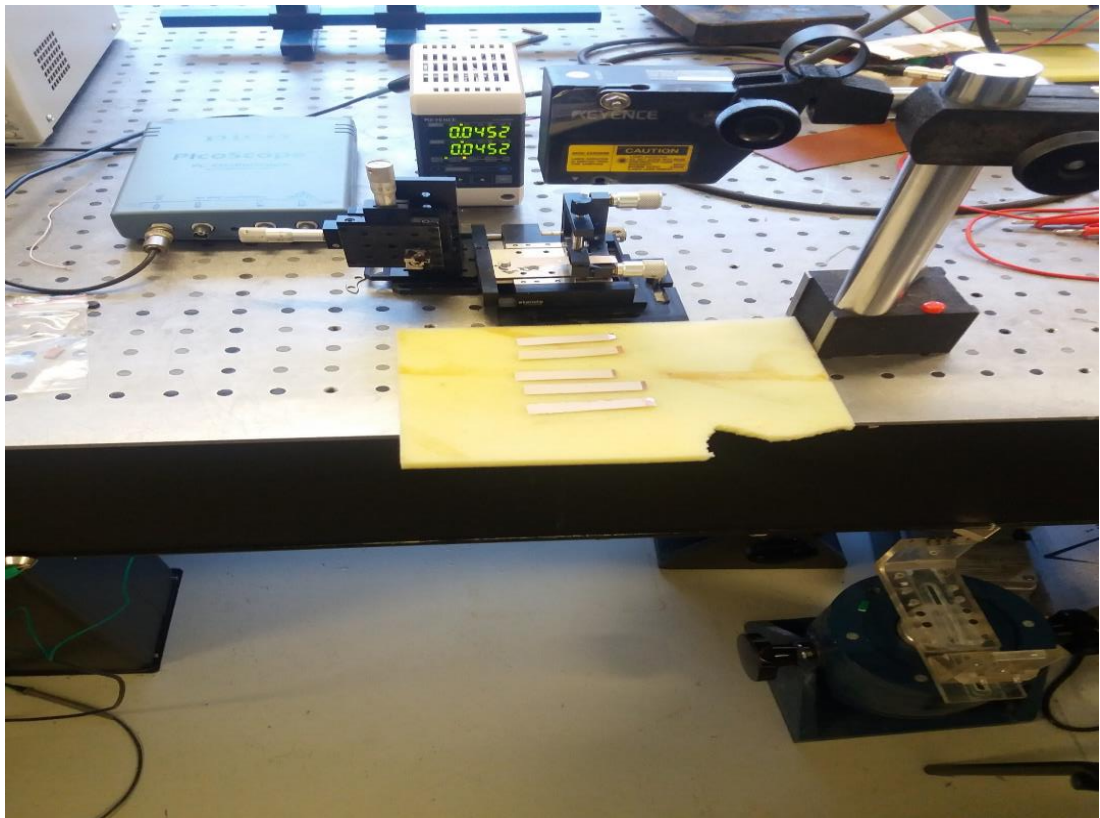


Figure 2-1 Experimental Setup

The Pico Scope collects signals from the accelerometer and PVEH. The signals from the Oscilloscope are sent to the Computer for processing using software. The experimental system was designed as a Mathematical pendulum. On indication, it provides a single impulse to the clamped element. Sensor head LK-G82, with an accuracy of 0.2 mm was used. The vibrations response was sensed and recorded using

a LASER triangulation displacement sensor LK-G3000 (Keyence, Illinois, USA). The measured data was collected with a data reading velocity of 5 Gs/s using the Data Acquisition PicoScope.

2.1 SPECIMEN PREPARATION

2.1.1 PZT Composite Fabrication

Lead Zirconate Titanate, with $x = 0.52$ in $[\text{Pb}(\text{Zr}_x, \text{Ti}_{1-x})\text{O}_3]$ or PZT (52/48) (herein after referred to as PZT) was prepared as an oxalic acid-water based Nano-powder. The chemical compositions used in preparing the PZT were lead (II) acetate $[\text{Pb}(\text{NO}_3)_2]$, titanium butoxide $[\text{Ti}(\text{C}_4\text{H}_9\text{O})_4]$, and zirconium butoxide $[\text{Zr}(\text{OC}_4\text{H}_9)_4]$ with reagents as oxalic acid, deionized water, acetic acid, and ammonia solution. The steps involved are as follows,

- Initially, 8.26 grams of Lead (II) acetate $[\text{Pb}(\text{NO}_3)_2]$ was taken and poured into 100 mL of water.
- Then, acetic acid was added to the solution and was heated to 50 °C so as to mix well and dissolve.
- In a separate glassware, 32 grams of oxalic acid was dissolved in 500 mL of water.
- 5.1 grams of Titanium butoxide and 7.65 grams of Zirconium butoxide was taken and added to the glassware with diluted Oxalic acid at a concentration of 80% and stirred well.
- Afterward the lead acetate solution was added to the glassware containing the mixture of titanium butoxide, zirconium butoxide and diluted oxalic acid solution.
- The final solution was alkalinized to a pH of 9-10 with 25% ammonia solution and was mixed for an hour.
- Afterward, the precipitate of the solution was washed with water and acetone during filtering in the vacuum.
- After filtering, the material was dried at 100 °C for 12 hours.
- The dried powder was then heated at 1000 °C for 9 hours.
- Finally, the heat dried PZT powder was milled finely to obtain Nano-powder.

2.2 PROCESS OF MAKING THE ELEMENT

Thus obtained Nano-powder was mixed with 20% solution of polyvinyl butyryl in benzyl alcohol. There were three defined conditions: 40% of PZT and 60% of the binding material, 60% of PZT and 40% of the binding material, 80% of PZT and 20% of the binding material. The purpose of using different PZT concentrations is the creation of piezoelectric materials with good piezoelectric characteristics and sufficient elasticity for imprinting a well-defined grating.

2.2.1 Screen printing technique

The pastes were prepared based on all three defined conditions and coated on a copper foil using a screen printing technique.

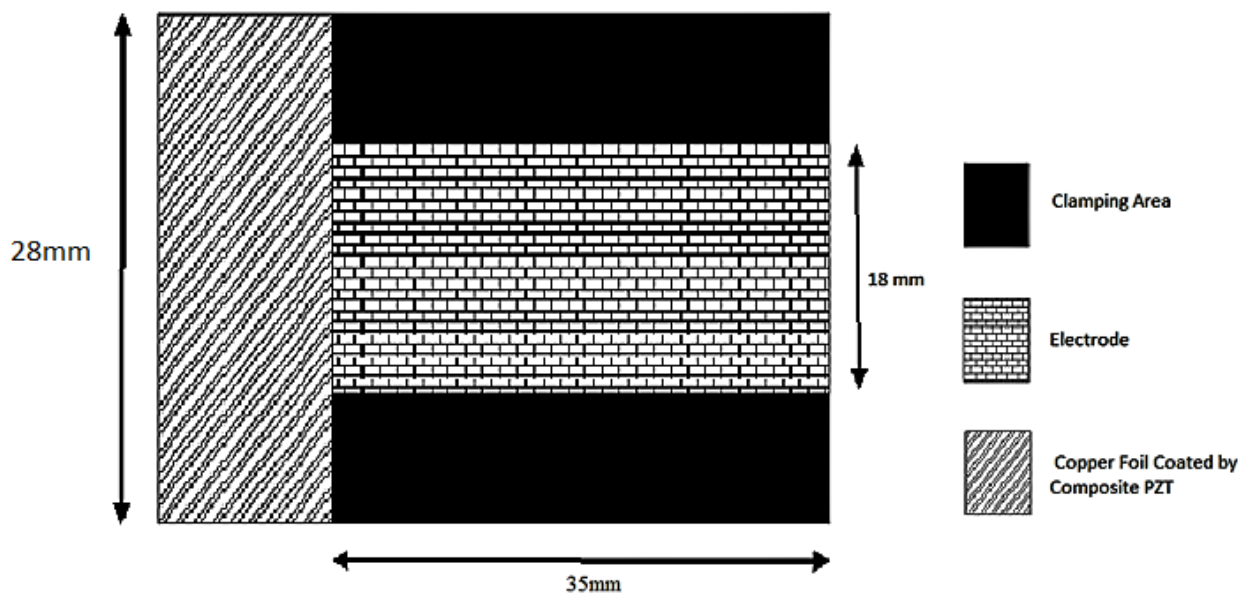


Figure 2-2 Plan of Piezoelectric Element

The screen printing was done using PZT paste on a 325 mesh of stainless steel and dried at 100 °C for 30 min. The advantage of this procedure is that it allows applying a smooth and equal thickness of the formed thin films (in this case, the thickness of all three elements was $\sim 1.2 \mu\text{m}$). Furthermore, a $4 \mu\text{m}$ periodical microstructure was formed on the top of the piezoelectric thin film by a hot embossing technique. Silver nanoparticles were formed from a solution of 0.05 M AgNO_3 in deionized water and dip-coated onto the periodical microstructure.

2.2 ELECTRICAL POLE ALIGNMENT

When an electric pulse was given to the microresonators containing PZT coating, an electrical pole alignment was achieved. This is done by measuring the generator voltage. This was achieved by a high voltage generator and a custom-made holder, within which the microresonator is placed as shown in the photoshoot below. A high voltage of 5 kV is provided for about 30 minutes. The Poling technique aligns positive and negative poles on either side of the PZT coated element. By doing so, the voltage characteristics of the PZT coating is improved.

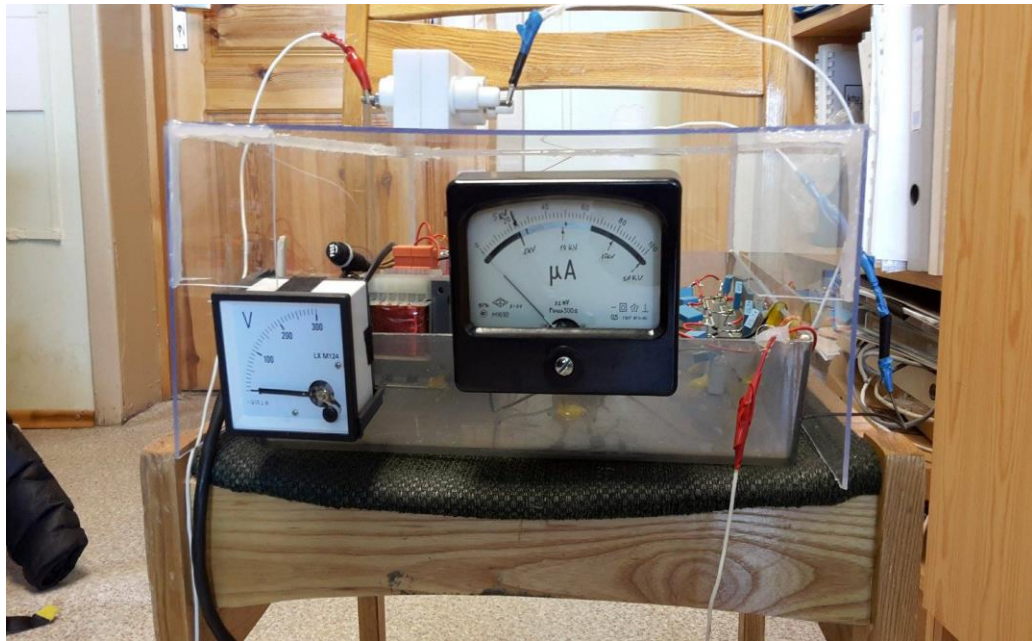


Figure 2-3 Pole Alignment Setup



Figure 2-4 Pole Alignment Setup

3.THEORETICAL CALCULATION

3.1 THEORETICAL CALCULATION WITH FORMULA

We assume that the PZT film coated beam element is fixed at one end while the other end is free. The origin of the coordinate axis is at the fixed end, point A. A typical beam of length 'L', width 'w', and thickness 't' is taken. The beam material is a copper film.

In a straight cantilever beam, under a vertical loading, the beam deforms into a curve. When the vertical loading is removed, the beam retains its original shape. However, the inertia of the beam will keep it in motion. The beam then vibrates at its characteristic frequencies. A thin PZT film is sputtered onto the beam, altering its flexural rigidity. This change, in turn, causes the frequency of vibrations to change. By measuring the frequency change, the film's Modulus of Elasticity can be calculated. We also assume that the Young's Modulus 'E' and Moment of Inertia 'I' are constant.

We know the dimensions of the data,

$$30 \text{ mm} \times 1.5 \text{ mm} \times 0.001 \text{ mm}$$

$$\text{Assuming the Young's Modulus } E = 4.2 \text{ GPa} = 4.2 \times 10^6 \text{ N/mm}^2$$

$$\text{Density of the element} = 6298 \text{ kg/m}^3 = 61.76 \times 10^{-6} \text{ N/mm}^3$$

$$\text{C/S Area, } A = 1.5 \times 0.001 \text{ mm}^2$$

$$\begin{aligned} \text{Moment of Inertia, } I &= 1.5 \times 0.001^3 / 12 \\ &= 1.25 \times 10^{-10} \text{ mm}^4 \end{aligned}$$

For a cantilever beam subjected to free vibration, and the system is considered as continuous system in which the beam mass is considered as distributed along with the stiffness of the shaft, the equation of motion can be written as

$$\frac{d^2}{dx^2} \left\{ EI(x) \frac{d^2 Y(x)}{dx^2} \right\} = \omega^2 m(x) Y(x) \quad (1)$$

We have following boundary conditions for a cantilever beam

$$x = 0, Y(x) = 0, \frac{dY(x)}{dx} = 0 \quad (2)$$

$$x = l, \frac{d^2Y(x)}{dx^2} = 0, \frac{d^3Y(x)}{dx^3} = 0 \quad (3)$$

For a uniform beam under free vibration from equation, we get

$$\frac{d^4Y(x)}{dx^4} - \beta^4 Y(x) = 0 \quad (4)$$

$$\beta^4 = \frac{\omega^2 m}{EI}$$

The mode shapes for a continuous cantilever beam is given as

$$f_n(x) = f_n(x) = A_n \{ (\sin \beta_n L - \sinh \beta_n L)(\sin \beta_n x - \sinh \beta_n x) + (\cos \beta_n L - \cosh \beta_n L)(\cos \beta_n x - \cosh \beta_n x) \} \quad (5)$$

$$n=1, 2, 3 \dots \infty \text{ and } \beta_n L = n\pi$$

A closed form of the circular natural frequency ω_{nf} , from above equation of motion and boundary conditions, can be written as,

$$\omega_n = \alpha_n^2 \sqrt{\frac{EI}{mL^4}} \quad (6)$$

$$\alpha_n = 1.875, 4.964, 7.885$$

$$f_n = \frac{K_n}{2\pi} \sqrt{\frac{EI g}{\omega l^4}} \quad (1 \text{ rad} = 1/2\pi \text{ Hz}) \quad (7)$$

Result

What is the X-section of the beam to be computed?

If circle, enter 1. If square, enter 2. If rectangle, enter 3

If your beam's X-section is not listed here, enter 4

To see example #1, hit ENTER or enter 0

To see example #2, enter 5

Enter your choice: 3

Enter Width of the X-section in [m]: 0.01

Enter Thickness of the X-section in [m]: 0.00004

Enter Length in [m]: 0.03

Material properties of the beam

Do you know your beam's material properties, viz. Young's modulus and density?

Enter 1, if you do; enter 0, if you don't: 1

Enter Young's modulus in [Pa]: 120000000000

Enter material density in [kg/m³]: 8960

How many modes and mode shapes would you like to evaluate?

Enter the number of modes and mode shapes to computed: 6

Mode shape # 1.000000 corresponds to nat. freq (fn): 26.274

Mode shape # 2.000000 corresponds to nat. freq (fn): 164.659

Mode shape # 3.000000 corresponds to nat. freq (fn): 461.051

Mode shape # 4.000000 corresponds to nat. freq (fn): 903.476

Mode shape # 5.000000 corresponds to nat. freq (fn): 1493.511

Mode shape # 6.000000 corresponds to nat. freq (fn): 2231.047

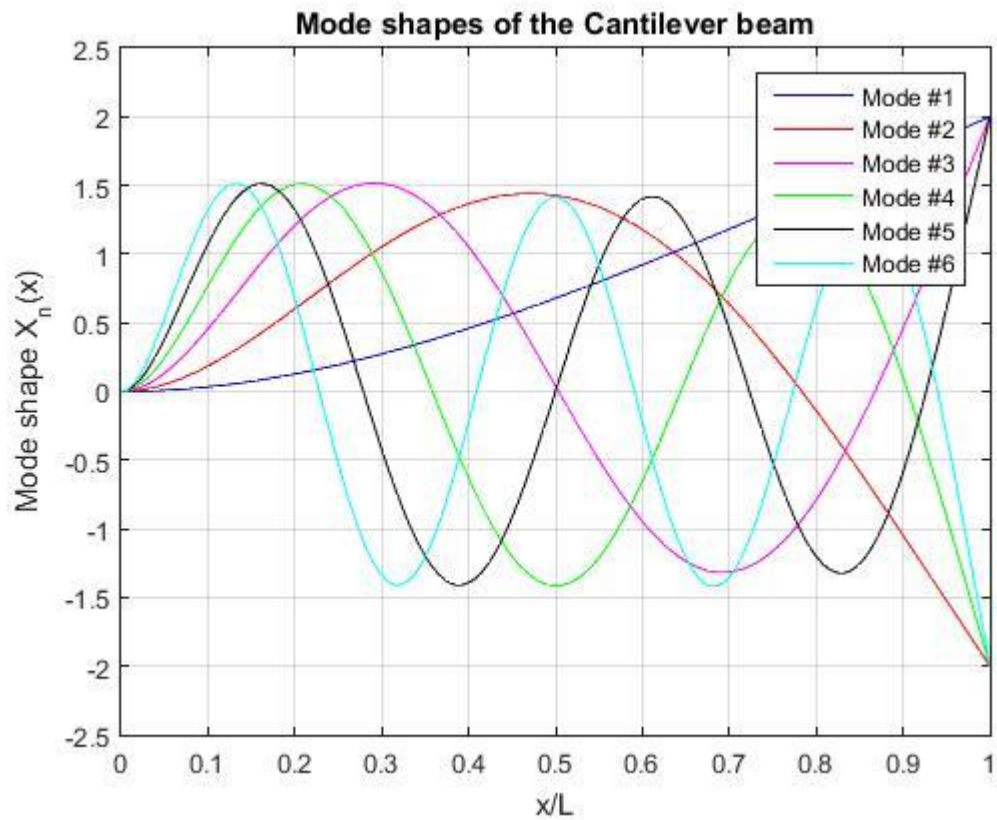


Figure 3-1 Mode shapes of cantilever beam

As time progresses, each mode will vibrate around the zero-displacement line with the frequency. The total beam motion is complex; each characteristic mode vibrates with a different size, shape, and frequency.

3.2 COMSOL Multiphysics

The PZT element is made as a Cantilever type. To analyze the possibility of effectively using a cantilever, its Finite Element model was developed

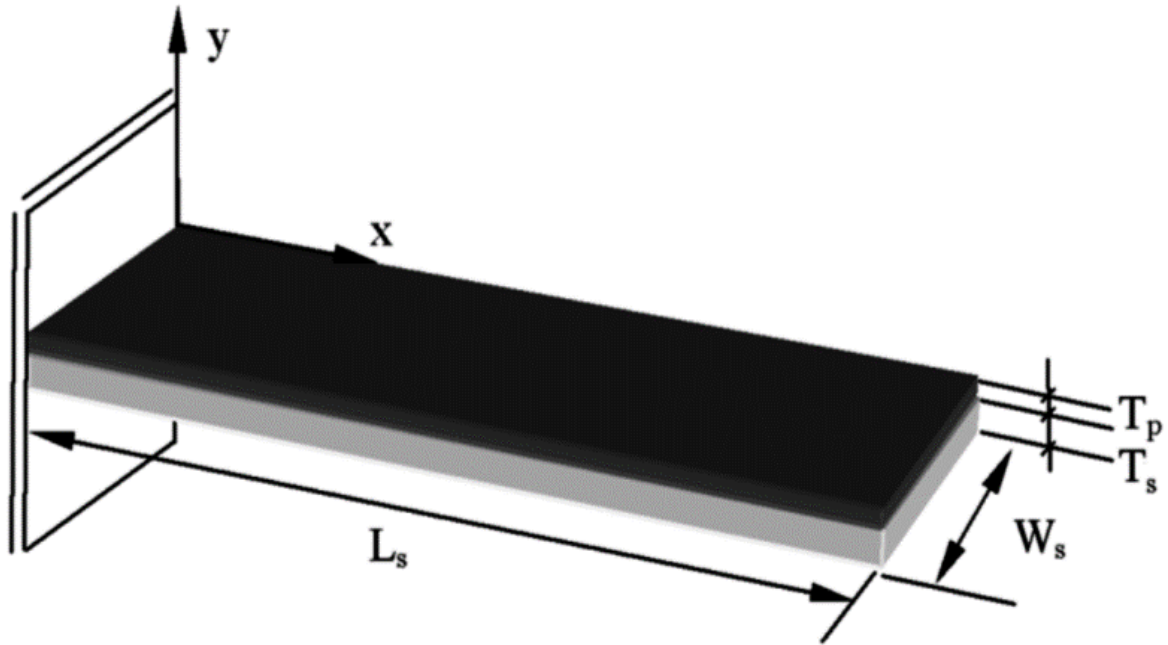


Figure 0-2 Model of rectangular cantilever beam

with the COSMOL Multiphysics software. Simulations were used to determine resonant frequencies, natural vibration modes as well as the preliminary location of the strain nodes of the vibrating structure. The figure above presents a scheme of the FE model which is based on a Copper rectangular cantilever beam ($L_s = 30$ mm, $T_s = 0.04$ mm, $W_s = 10$ mm) with one piezoelectric layer bonded on its top surface ($L_p = 30$ mm, $T_p = 0.05$ mm, $W_p = 10$ mm).

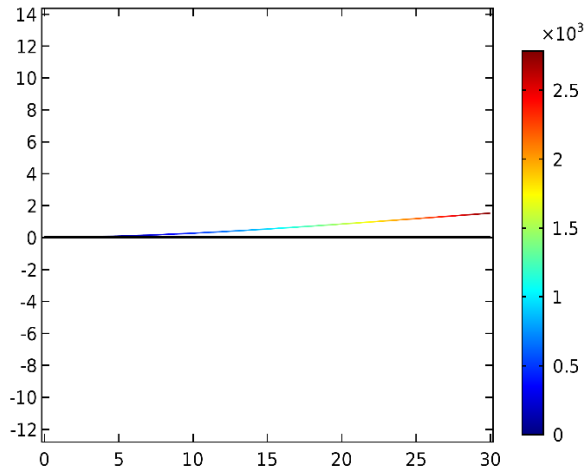
For modelling of the cantilever beam, piezoelectric modules of COMSOL were selected. These modules involve the studies based on eigenfrequency, time dependent, and customized analysis. Each study involves the formation of the set of equations by applying appropriate boundary conditions to the developed model.

The properties of materials used in the modelling,

S. No	Material Name	Density (kg/m ³)	Poisson's Ratio	Young's Modulus (Pa)
1	Copper (Cu)	8960	0.34	120e9
2	Lead Zirconate Titanate (PZT)	6298	0.3	4.2e9

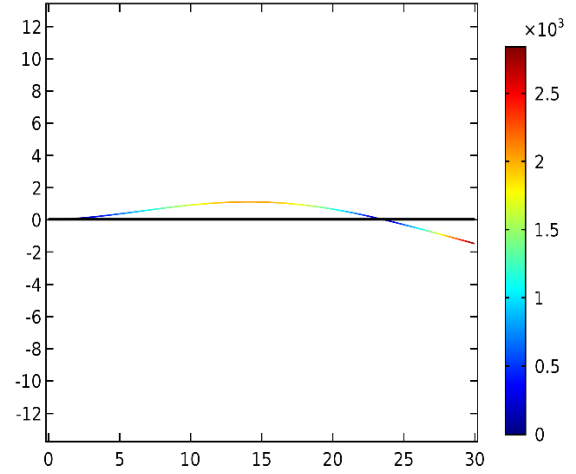
Table 1 Properties of the materials

Eigenfrequency=26.487 Hz Surface: Total displacement (mm)



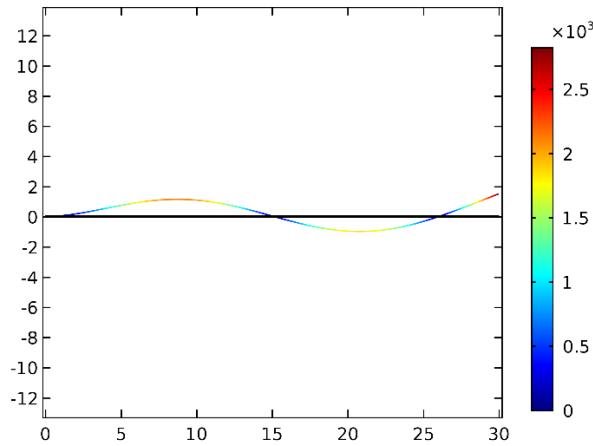
(a)

Eigenfrequency=165.88 Hz Surface: Total displacement (mm)



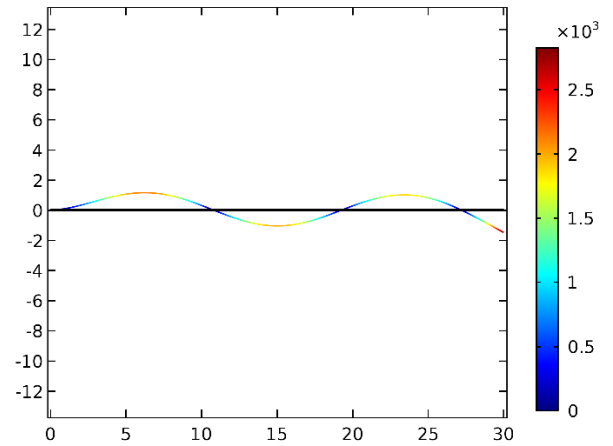
(b)

Eigenfrequency=464.44 Hz Surface: Total displacement (mm)



(c)

Eigenfrequency=910.05 Hz Surface: Total displacement (mm)



(d)

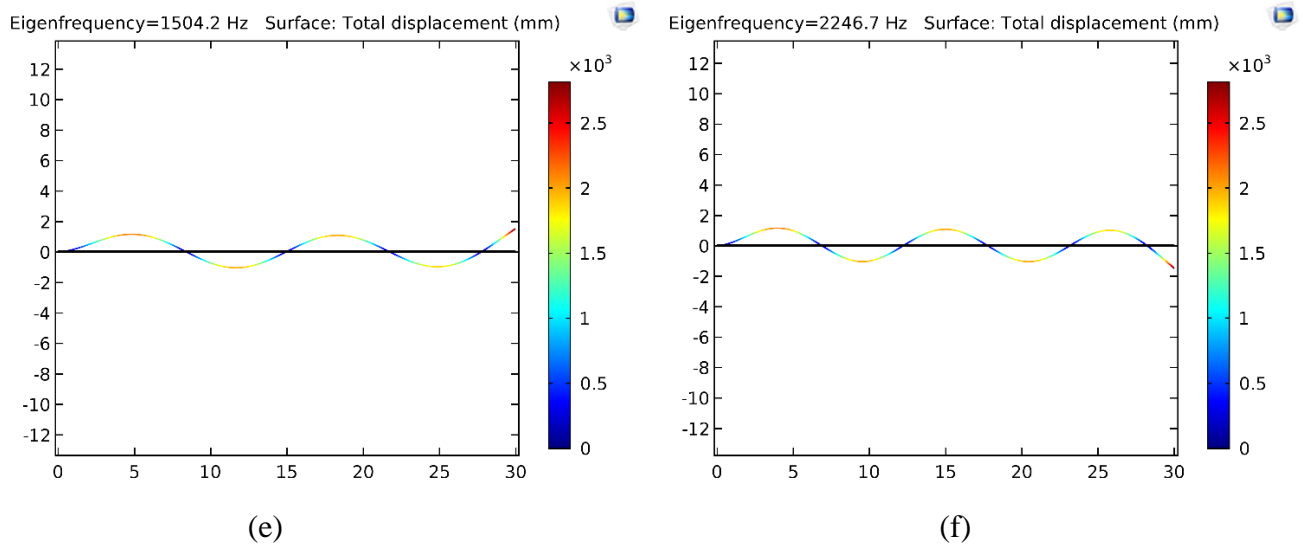


Figure 3-3 Modelling of PZT Composite material using COMSOL Multiphysics

The structural mechanics module was selected to perform the eigenfrequency analysis. The parameters of cantilever beam were selected and appropriate boundary conditions were applied. The developed model calculates six eigenfrequencies.

3.3 Comparison of Theoretical and Experimental Results

S. No	FEM Modelling using COMSOL (Hz)	Analytical Calculation (Hz)	Error
1	26.487	26.274	0.213
2	165.88	164.659	1.221
3	464.44	461.051	3.389
4	910.05	903.476	6.574
5	1504.2	1493.511	10.689
6	2246.7	2231.047	15.653

Table 2 Comparison table of eigen frequencies for experimental and analytical results

In this comparison table the eigenfrequency values that has been obtained during the simulation of Finite element modelling for the cantilever beam using COMSOL Multiphysics software, and the theoretical values which were obtained by calculating through deriving formulas have been added. The analytical frequencies were calculated using the equation (7). Table 2 shows the error between simulated and analytically calculated eigenfrequencies.

4.RESULTS

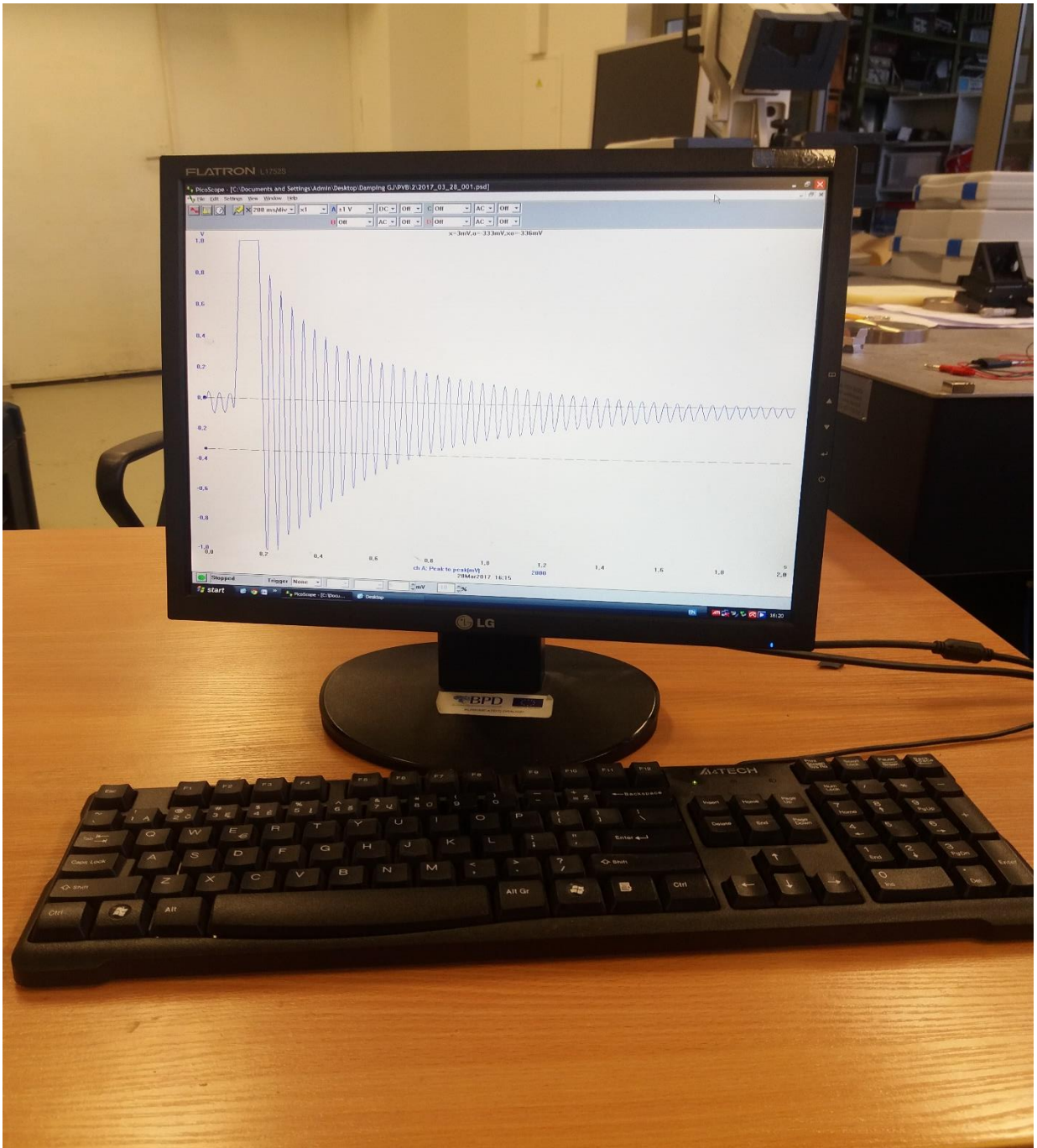


Figure 4-1 Frequency analysis

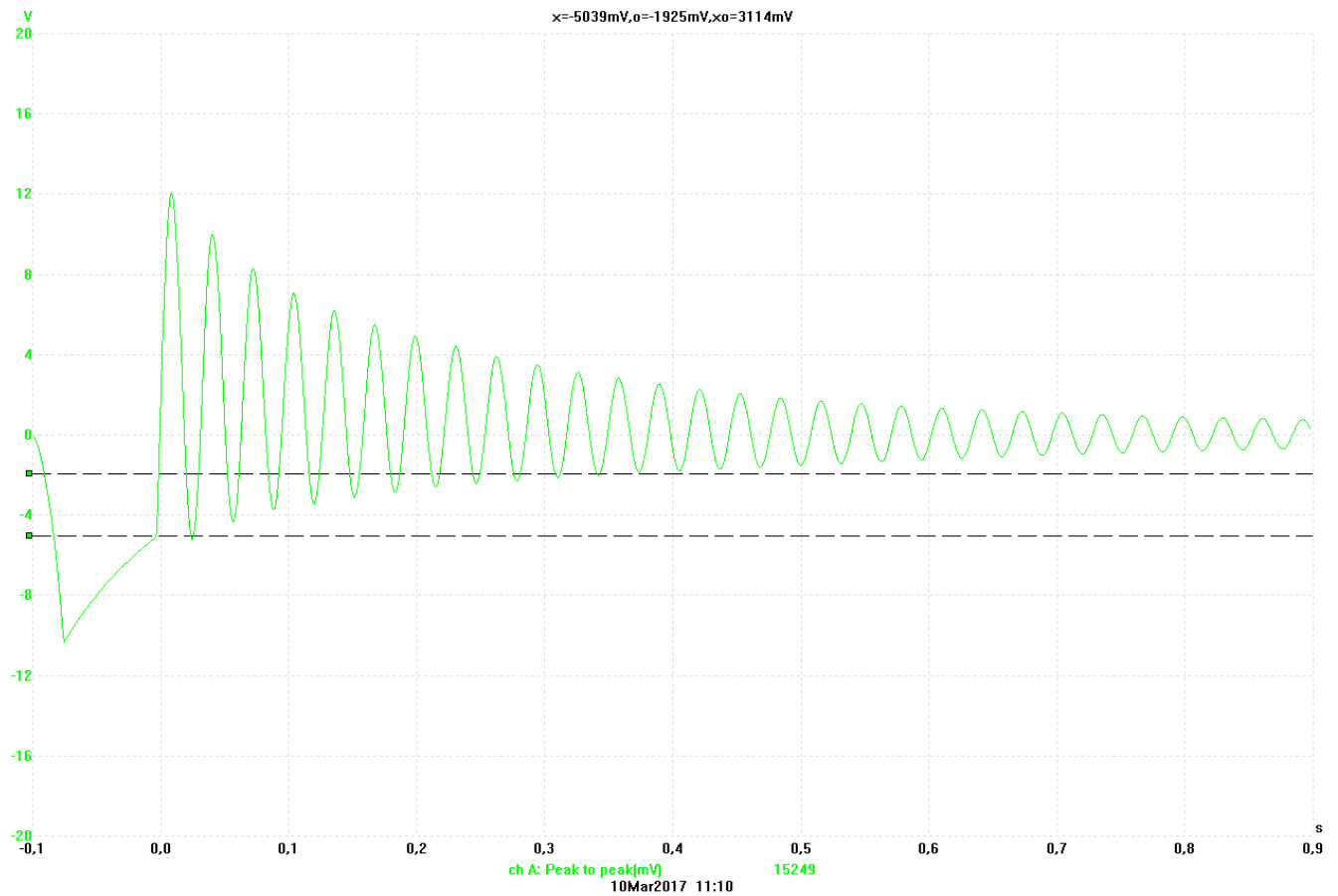


Figure 4-2 Vibrational analysis

Fig 4.2 shows the settling time of cantilever beam. The free end of the singly clamped cantilever to set an initial deflection. For instance, Here the cantilever tip bends down initially, by controlling the translational stage. As the positioner tip is abruptly retracted laterally, the cantilever is released and oscillations are generated, as illustrated in Fig. 4.2.

Thus, in this, the settling time of the deflection in the beam can be rested approximately 1.5s.

5.CONCLUSIONS

1. The theoretical eigenfrequencies of the created samples has been measured and the calculation has been done using the MATLAB software to analyze the different mode and the obtained frequencies 26.274 for the first mode and 2231.047 for the sixth mode.
2. Several simulations were carried out with developed model in COMSOL, and as a result we got the initial frequency from 26.487 and the final frequency of 2246.7 which will be compared with the theoretical results.
3. The analytical results of eigen frequency were compared with results obtained from the model. Modal analysis showed that the comparison of natural frequencies obtained from analytical and COMSOL are having a close match differing Error from the minimum of 0.213 and the maximum up to 15.653 as for the 6 modes of frequencies.

REFERENCES

1. A, E., M, K., S, S., & A, B. (2004). Modelling the flexural behaviour of sandwich compositematerials under cyclic fatigue. *Materials and Design*, 199-208.
2. ACTION, N., ALBERT, C., & PEARSON, L. (2012). Finite Element Modeling of a Piezoelectric Composite Beam and Comparative Performance Study of Piezoelectric Materials for Voltage Generation. *Materials Science*.
3. APC International, L. (2016). *Knowledge Center*. Retrieved from americanpiezo.com: <https://www.americanpiezo.com/piezo-theory/pzt.html>
4. B, H., G, H., A, G., A, M., & R, F. (2000). *COMPARISON OF DIFFERENT PIEZOELECTRIC MATERIALS FOR THE DESIGN OF EMBEDDED TRANSDUCERS FOR STRUCTURAL HEALTH MONITORING APPLICATIONS*. PUERTO RICO: ULTRASONICS SYMPOSIUM.
5. B, R., D, T., M, B., T, S., & J, F. (2011). Electromagnetic and Thermal Modeling of Composite MaterialsUsing Multilayer Shell Elements. *IEEE TRANSACTIONS ON MAGNETICS*, 1134-1137.
6. BARSCHKE, M., URIBE, D., RUIZ, O. E., JENSEN, J., & LOPEZ, C. (2009). Finite Element Modeling of Composite. *Ingeniería y Ciencia*, 133-153.
7. BEHROUZ, S., & KHALIL, N. (2015). EFFECT OF SUBSTRATE THICKNESS ON QUALITY FACTOR OF MECHANICAL RESONATORS. *INERTIAL SENSORS AND SYSTEMS*, 1-4.
8. BIQIN, D., CHENG , S., & HAO, Z. F. (2017). OPTICAL DETECTION OF ULTRASOUND IN PHOTOACOUSTIC IMAGING. *BIOMEDICAL ENGINEERING IEEE TRANSACTIONS*, 4-15.
9. CeramTec. (2017). *Products*. Retrieved from ceramtec.com: <https://www.ceramtec.com/competence/pzt-electro-ceramics/>
10. Dineva, P., Gross, D., Muller, R., & Rangelov, T. (2014). Types of Piezoelectric Materials. In P. Dineva, D. Gross, R. Muller, & T. Rangelov, *Dynamic fracture of piezoelectric materials: Solution of time-harmonic problems via biem* (p. 10). London: Springer International Publishing. doi:10.1007/978-3-319-03961-9
11. E, E., & E.L, P. (2014, Sep-Oct). Finite element analysis of different composite materials using multi continuum method. *IOSR Journal of Mechanical and Civil Engineering*, 11(5), 94-99. Retrieved from www.iosrjournals.org/iosr-jmce/papers/vol11-issue5/Version-5/N011559499.pdf
12. E, V., B, S., P R, V., & M S , V. (2001). PIEZOELECTRIC PROPERTIES OF FERROELECTRIC PZT-POLYMER COMPOSITES. *JOURNAL OF PHYSICS D:APPLIED PHYSICS*, 4.
13. GHOSE, B., BALASUBRAMANIAM, K., C V, K., & A, S. (2011). *COMSOL® BASED 2-D FEM MODEL FOR ULTRASONIC GUIDED WAVE PROPAGATION IN SYMMETRICALLY*

DELAMINATED UNIDIRECTIONAL MULTILAYERED COMPOSITE STRUCTURE.
CHENNAI.

14. Joe. (2009). *Sensors - Piezoelectric Ceramic & Film*. Retrieved from sensorwiki.org: http://www.sensorwiki.org/doku.php/sensors/piezoelectric_ceramic_film
15. K, N., & T, S. (2009). Modelling of ‘thermal shocks’ in composite materials using a meshfree fem. *Computational Materials Science*, 44(4), 1307-1311. doi:<https://doi.org/10.1016/j.commatsci.2008.08.019>
16. Lerman, M., & Elata, D. (2010). On the quality-factor of micro-resonators. *Proc. Eurosensors XXIV*,. 5, pp. 1-3. Linz: Elsevier Ltd. doi:<https://doi.org/10.1016/j.proeng.2010.09.056>
17. LERMAN, M., & ELATA, D. (2010). ON THE QUALITY-FACTOR OF MICRO-RESONATORS. *PROCEDIA ENGINEERING*, 1-3.
18. LOAN, I. A., MICKY , R., JOEL, A., ROGER, B., NICOLAS, C., & PHILIPPE, L. (2010). COMPARATIVE MATERIAL STUDY BETWEEN PZT CERAMIC AND NEWER CRYSTALLINE PMN-PT AND PZN-PT MATERIALS FOR COMPOSITE BIMORPH ACTUATORS. *MATERIAL SCIENCE*, 1-9.
19. LUIZ, M. F., JOSE, Q. D., & ILHA , S. (2003). Study of Pyroelectric Activity of PZT/PVDF-HFP Composite. *MATERIALS RESEARCH*, 469-473.
20. M.L, G., YU.A, D., D.F, Z., V.N, K., YU.M, Z., & V.L, L. (2015). High-Q Factor Optical Whispering-Gallery Mode Microresonators and Their Use in Precision Measurements. *MEASUREMENT TECHNIQUES*, 1386-1395.
21. MATTHEW, H. W. (1998). EXPERIMENTAL PROCEDURE. *PROPERTIES OF PZT-BASED PIEZOELECTRIC CERAMICS BETWEEN-150 AND 250°C*, 2-22.
22. MICHAEL, L., & DAVID, E. (2010). ON THE QUALITY-FACTOR OF MICRO-RESONATORS. *PROCEDIA ENGINEERING*, 95-98.
23. Mohammadi, M. (2013). A comparison between quartz and pzt ceramic for sensoric applications. *Research Desk - Review Article*, 323-324. Retrieved from [researchdesk.net/rdadmin/rd_files/Research Desk, 2013, Oct-Dec 2\(4\). 321-325 .pdf](http://researchdesk.net/rdadmin/rd_files/Research%20Desk,%202013,%20Oct-Dec%202(4).321-325.pdf)
24. N.K, J. (2015). *Piezoelectric and dielectric properties of polymer-ceramic composites for sensors*, 3-8.
25. PG, B., & SR, H. (n.d.). *FINITE ELEMENT MODELLING OF 3D WOVEN COMPOSITES FOR STIFFNESS PREDICTION*. Queens Building.
26. S, B., & F, B. (2008). PIEZOELECTRIC POLYMERS AND THEIR APPLICATIONS. *PIEZOELECTRICITY*, 157-177.
27. SAS IP, I. (2017). *Software - Ansys*. Retrieved from [sharcnet.ca: https://www.sharcnet.ca/Software/Ansys/17.0/en-us/help/ans_elem/Hlp_E_SOLSH190.html](https://www.sharcnet.ca/Software/Ansys/17.0/en-us/help/ans_elem/Hlp_E_SOLSH190.html)
28. T, D., & S, A. P. (n.d.). *slideshare.net*. Retrieved from [slideshare.net: https://www.slideshare.net/dheepseela/a-study-of-electromechanical-behavior-of-piezo-](https://www.slideshare.net/dheepseela/a-study-of-electromechanical-behavior-of-piezo-)

ceramic-smart-materials-and-application-of-piezo-ceramic-pzt-for-vibration-alerts-in-mobile-phones

29. Wangikar, K. S., Jadhav, S., & Patil, V. (2014). Literature review on modelling and finite element analysis of delamination of composite. *International Journal of Engineering Development and Research*, 2(1), 254-261. Retrieved from <https://www.ijedr.org/papers/IJEDR1401043.pdf>

Appendix

Matlab Code

`function Cbeam(~)`


```

L=.321;
W=.05;
Th=.006;
A=W*Th;
V=L*W*Th;
Ix=(1/12)*W*Th^3;
Iy=(1/12)*(W^3)*Th;
E=69.90e+9;
Ro=2770;
elseif CS==1
    R=input('Enter Radius of the X-section: ');
    L=input('Enter Length: ');
    Ix=(1/4)*pi*R^4;
    Iy=Ix;
    A=pi*R^2;
    disp('Material properties of the beam')
    display('Do you know your beam"s material properties, viz. Young"s modulus and density ?')
    YA=input('Enter 1, if you do; enter 0, if you don"t ');
    if YA==1
        E=input('Enter Young"s modulus in [Pa]: ');
        Ro=input('Enter material density in [kg/m^3]: ');
    else
        display('Steel: E=2.1e+11 [Pa]; Ro=7850 [Kg/m^3]')
        display('Copper: E=1.2e+11 [Pa]; Ro=8933 [Kg/m^3]')
        display('Aluminum: E=0.69e+11 [Pa]; Ro=2700 [Kg/m^3]')
        E=input('Enter Young"s modulus in [Pa]: ');
        Ro=input('Enter material density in [kg/m^3]: ');
    end
elseif CS==2
    W=input('Enter Width of the X-section in [m]: ');
    L=input('Enter Length in [m]: ');
    Ix=(1/12)*W^4;

```

```

A=W^2;
disp('Material properties of the beam');
disp('Do you know your beam"s material properties, viz. Young"s modulus and density ?')
YA=input('Enter 1, if you do; enter 0, if you don"t: ');
if YA==1
E=input('Enter Young"s modulus in [Pa]: ');
Ro=input('Enter material density in [kg/m^3]: ');
else
    display('Steel: E=2.1e+11 [Pa]; Ro=7850 [Kg/m^3]')
    display('Copper: E=1.2e+11 [Pa]; Ro=8933 [Kg/m^3]')
    display('Aluminum: E=0.69e+11 [Pa]; Ro=2700 [Kg/m^3]')
    E=input('Enter Young"s modulus in [Pa]: ');
    Ro=input('Enter material density in [kg/m^3]: ');
end
elseif CS==3
W=input('Enter Width of the X-section in [m]: ');
Th=input('Enter Thickness of the X-section in [m]:');
L=input('Enter Length in [m]: ');
Ix=(1/12)*W*Th^3;
Iy=(1/12)*(W^3)*Th;
A=W*Th;
disp('Material properties of the beam')
disp('Do you know your beam"s material properties, viz. Young"s modulus and density ?')
YA=input('Enter 1, if you do; enter 0, if you don"t: ');
if YA==1
E=input('Enter Young"s modulus in [Pa]: ');
Ro=input('Enter material density in [kg/m^3]: ');
else
    display('Steel: E=2.1e+11 [Pa]; Ro=7850 [Kg/m^3] ')
    display('Copper: E=1.2e+11 [Pa]; Ro=8933 [Kg/m^3] ')
    display('Aluminum: E=0.69e+11 [Pa]; Ro=2700 [Kg/m^3] ')
    E=input('Enter Young"s modulus in [Pa]: ');

```

```

    Ro=input('Enter material density in [kg/m^3]: ');
end
elseif CS==4
    display('Note: you need to compute Ix (area moment of inertia along x axis) and X-sectional area')
    L=input('Enter Length in [m]: ');
    Ix=('Enter Ix in [m^4]: ');
    A=('Enter X-sectional area in [m^2]: ');
    disp('Material properties of the beam')
    disp('Do you know your beam"s material properties, viz. Young"s modulus and density ?')
    YA=input('Enter 1, if you do; enter 0, if you don"t ');
    if YA==1
        E=input('Enter Young"s modulus in [Pa]: ');
        Ro=input('Enter material density in [kg/m^3]: ');
    else
        display('Steel: E=2.1e+11 Pa; Ro=7850 Kg/m^3 ')
        display('Copper: E=1.2e+11 Pa; Ro=8933 Kg/m^3 ')
        display('Aluminum: E=0.69e+11 Pa; Ro=2700 Kg/m^3 ')
        E=input('Enter Young"s modulus in [Pa]: ');
        Ro=input('Enter material density in [kg/m^3]: ');
    end
elseif CS==5
    display('Example #2')
    display('This is a rectangular X-sectional steel beam ')
    display('Length=0.45 m; Width=0.04 m; Thickness=0.003 m;')
    L=.45; W=.04; Th=.003;
    A=W*Th;
    Ix=(1/12)*W*Th^3;
    E=2.1*1e11; Ro=7.85*1e3;
else
    F=warndlg('It is not clear what your choice of X-section of a beam is. Re-run the script and enter
your beam"s X-section !!!,!! Warning !!');
    waitfor(F)
end

```

```

display('Type in:>> Cbeam')
pause(3)
return
end

display('How many modes and mode shapes would you like to evaluate ?')
HMMS=input('Enter the number of modes and mode shapes to computed: ');
if HMMS>=7
    disp(' ')
    warning('NOTE: Up to 6 mode shapes (plots) are displayed via the script. Yet, using evaluated data
(Xnx) of the script, more mode shapes can be plotted');
    disp(' ')
end
Nm=3*HMMS;
jj=1;
while jj<=Nm;
    betaNL(jj)=fzero(@(betaNL)cosh(betaNL)*cos(betaNL)+1,[jj jj+3]);
    jj=jj+3;
end

index=(betaNL~=0);
betaNLall=(betaNL(index));
%fprintf('betaNL value is %2.3f\n', betaNLall);
betaN=(betaNLall/L);
k=1;
wn=ones(1,length(betaN));
fn=ones(1,length(wn));
while k<=length(betaN);
    wn(k)=betaN(k)^2*sqrt((E*Ix)/(Ro*A));
    fn(k)=wn(k)/(2*pi);
    fprintf('Mode shape # %2f corresponds to nat. freq (fn): %3.3f\n', k, fn(k) );
    k=k+1;
end

```

```

end

x=linspace(0, L, 180);
xl=x./L;
sigmaN=zeros(1, HMMS);
for ii=1:HMMS;
    sigmaN(ii)=(sinh(betaN(ii)*L)-sin(betaN(ii)*L))/(cosh(betaN(ii)*L)+cos(betaN(ii)*L));
end
Tc='(cosh(betaN(ii).*x(jj))-cos(betaN(ii).*x(jj)))-sigmaN(ii).*(sinh(betaN(ii).*x(jj))-
sin(betaN(ii).*x(jj)))';
Xnx=zeros(length(betaN),length(x));

for ii=1:length(betaN)
    for jj=1:length(x)
        Xnx(ii,jj)=eval(Tc);
    end
end
end
% Plot mode shapes;

MMS=HMMS;
if MMS==1
    plot(xl,Xnx(1,:), 'b-')
    title('Mode shape of the Cantilever beam')
    legend('Mode #1', 0); xlabel('x/L'); ylabel('Mode shape X_n(x)'); grid
    hold off
elseif MMS==2
    plot(xl,Xnx(1,:), 'b-'); hold on
    plot(xl,Xnx(2,:), 'r-');grid
    title('Mode shapes of the Cantilever beam')
    legend('Mode #1', 'Mode #2', 0)
    xlabel('x/L'); ylabel('Mode shape X_n(x)')
    hold off;

```

```

elseif MMS==3
    plot(xl,Xnx(1,:), 'b-'); hold on
    plot(xl,Xnx(2,:), 'r-')
    plot(xl,Xnx(3,:), 'm-');grid
    title('Mode shapes of the Cantilever beam')
    legend('Mode #1', 'Mode #2', 'Mode #3', 0)
    xlabel('x/L'); ylabel('Mode shape X_n(x)')
    hold off;
elseif MMS==4
    plot(xl,Xnx(1,:), 'b-'); hold on
    plot(xl,Xnx(2,:), 'r-')
    plot(xl,Xnx(3,:), 'm-')
    plot(xl,Xnx(4,:), 'c-'); grid
    title('Mode shapes of the Cantilever beam')
    legend('Mode #1', 'Mode #2', 'Mode #3', 'Mode #4', 0)
    xlabel('x/L'); ylabel('Mode shape X_n(x)')
    hold off;
elseif MMS==5
    plot(xl,Xnx(1,:), 'b-'); hold on
    plot(xl,Xnx(2,:), 'r-')
    plot(xl,Xnx(3,:), 'm-')
    plot(xl,Xnx(4,:), 'g-')
    plot(xl,Xnx(5,:), 'k-')
    grid
    title('Mode shapes of the Cantilever beam')
    legend('Mode #1', 'Mode #2', 'Mode #3', 'Mode #4', 'Mode #5', 0)
    xlabel('x/L'); ylabel('Mode shape X_n(x)')
    hold off
elseif MMS>=6
    plot(xl,Xnx(1,:), 'b-'); hold on
    plot(xl,Xnx(2,:), 'r-')
    plot(xl,Xnx(3,:), 'm-')

```

```

plot(xl,Xnx(4,:), 'g-')
plot(xl,Xnx(5,:), 'k-')
plot(xl,Xnx(6,:), 'c-')
grid
title('Mode shapes of the Cantilever beam')
legend('Mode #1', 'Mode #2', 'Mode #3', 'Mode #4', 'Mode #5','Mode #6', 0)
xlabel('x/L'); ylabel('Mode shape X_n(x)')
hold off

```

end

end

Comsol Multiphysics

solid.rho	material.rho	kg/m ³	Density	Domains 1–2
solid.Qh	0	W/m ³	Total power dissipation density	Domains 1–2

uTXt	uTXTIME	1/s	Tangential gradient of u, X component, first time derivative	Boundaries 1–7
uTYt	uTYTIME	1/s	Tangential gradient of u, Y component, first time derivative	Boundaries 1–7
uTXtt	uTXTIMETIME	1/s ²	Tangential gradient of u, X component, second time derivative	Boundaries 1–7
uTYtt	uTYTIMETIME	1/s ²	Tangential gradient of u, Y component, second time derivative	Boundaries 1–7
uXt	uXTIME	1/s	Gradient of u, X component, first time derivative	Domains 1–2
uYt	uYTIME	1/s	Gradient of u, Y component, first time derivative	Domains 1–2
uXtt	uXTIMETIME	1/s ²	Gradient of u, X component, second time derivative	Domains 1–2
uYtt	uYTIMETIME	1/s ²	Gradient of u, Y component, second time derivative	Domains 1–2
vTXt	vTXTIME	1/s	Tangential gradient of v, X component, first time derivative	Boundaries 1–7
vTYt	vTYTIME	1/s	Tangential gradient of v, Y component, first time derivative	Boundaries 1–7
vTXtt	vTXTIMETIME	1/s ²	Tangential gradient of v, X component, second time derivative	Boundaries 1–7
vTYtt	vTYTIMETIME	1/s ²	Tangential gradient of v, Y component,	Boundaries 1–7

			second time derivative	
vXt	vXTIME	1/s	Gradient of v, X component, first time derivative	Domains 1–2
vYt	vYTIME	1/s	Gradient of v, Y component, first time derivative	Domains 1–2
vXtt	vXTIMETIME	1/s ²	Gradient of v, X component, second time derivative	Domains 1–2
vYtt	vYTIMETIME	1/s ²	Gradient of v, Y component, second time derivative	Domains 1–2
ut	uTIME	m/s	Structural velocity field, X component	Domains 1–2
vt	vTIME	m/s	Structural velocity field, Y component	Domains 1–2
utt	uTIMETIME	m/s ²	Acceleration field, X component	Domains 1–2
vtt	vTIMETIME	m/s ²	Acceleration field, Y component	Domains 1–2
solid.gradUxX	uX	1	Displacement gradient, xX component	Domains 1–2
solid.gradUyX	vX	1	Displacement gradient, yX component	Domains 1–2
solid.gradUzX	0	1	Displacement gradient, zX component	Domains 1–2
solid.gradUxY	uY	1	Displacement gradient, xY component	Domains 1–2
solid.gradUyY	vY	1	Displacement gradient, yY component	Domains 1–2
solid.gradUzY	0	1	Displacement gradient, zY component	Domains 1–2
solid.gradUxZ	0	1	Displacement gradient, xZ component	Domains 1–2

solid.gradUyZ	0	1	Displacement gradient, yZ component	Domains 1–2
solid.gradUzZ	0	1	Displacement gradient, zZ component	Domains 1–2
solid.FdxX	1+solid.gradUxX	1	Deformation gradient, xX component	Domains 1–2
solid.FdyX	solid.gradUyX	1	Deformation gradient, yX component	Domains 1–2
solid.FdzX	solid.gradUzX	1	Deformation gradient, zX component	Domains 1–2
solid.FdxY	solid.gradUxY	1	Deformation gradient, xY component	Domains 1–2
solid.FdyY	1+solid.gradUyY	1	Deformation gradient, yY component	Domains 1–2
solid.FdzY	solid.gradUzY	1	Deformation gradient, zY component	Domains 1–2
solid.FdxZ	solid.gradUxZ	1	Deformation gradient, xZ component	Domains 1–2
solid.FdyZ	solid.gradUyZ	1	Deformation gradient, yZ component	Domains 1–2
solid.FdzZ	1+solid.gradUzZ	1	Deformation gradient, zZ component	Domains 1–2
solid.Fdlx1	solid.FdxX	1	Deformation gradient, local, x1 component	Domains 1–2
solid.Fdly1	solid.FdyX	1	Deformation gradient, local, y1 component	Domains 1–2
solid.Fdlz1	solid.FdzX	1	Deformation gradient, local, z1 component	Domains 1–2
solid.Fdlx2	solid.FdxY	1	Deformation gradient, local, x2 component	Domains 1–2
solid.Fdly2	solid.FdyY	1	Deformation gradient, local, y2 component	Domains 1–2

solid.Fdlz2	solid.FdzY	1	Deformation gradient, local, z2 component	Domains 1–2
solid.Fdlx3	solid.FdxZ	1	Deformation gradient, local, x3 component	Domains 1–2
solid.Fdly3	solid.FdyZ	1	Deformation gradient, local, y3 component	Domains 1–2
solid.Fdlz3	solid.FdzZ	1	Deformation gradient, local, z3 component	Domains 1–2
solid.D11	$\text{solid.E} * (1 - \text{solid.nu}) / ((1 + \text{solid.nu}) * (1 - 2 * \text{solid.nu}))$	Pa	Elasticity matrix, 11 component	Domains 1–2
solid.D12	$\text{solid.E} * \text{solid.nu} / ((1 + \text{solid.nu}) * (1 - 2 * \text{solid.nu}))$	Pa	Elasticity matrix, 12 component	Domains 1–2
solid.D13	$\text{solid.E} * \text{solid.nu} / ((1 + \text{solid.nu}) * (1 - 2 * \text{solid.nu}))$	Pa	Elasticity matrix, 13 component	Domains 1–2
solid.D14	0	Pa	Elasticity matrix, 14 component	Domains 1–2
solid.D15	0	Pa	Elasticity matrix, 15 component	Domains 1–2
solid.D16	0	Pa	Elasticity matrix, 16 component	Domains 1–2
solid.D22	$\text{solid.E} * (1 - \text{solid.nu}) / ((1 + \text{solid.nu}) * (1 - 2 * \text{solid.nu}))$	Pa	Elasticity matrix, 22 component	Domains 1–2
solid.D23	$\text{solid.E} * \text{solid.nu} / ((1 + \text{solid.nu}) * (1 - 2 * \text{solid.nu}))$	Pa	Elasticity matrix, 23 component	Domains 1–2
solid.D24	0	Pa	Elasticity matrix, 24 component	Domains 1–2
solid.D25	0	Pa	Elasticity matrix, 25 component	Domains 1–2
solid.D26	0	Pa	Elasticity matrix, 26 component	Domains 1–2
solid.D33	$\text{solid.E} * (1 - \text{solid.nu}) / ((1 + \text{solid.nu}) * (1 - 2 * \text{solid.nu}))$	Pa	Elasticity matrix, 33 component	Domains 1–2
solid.D34	0	Pa	Elasticity matrix, 34 component	Domains 1–2
solid.D35	0	Pa	Elasticity matrix, 35 component	Domains 1–2
solid.D36	0	Pa	Elasticity matrix, 36 component	Domains 1–2
solid.D44	$0.5 * \text{solid.E} / (1 + \text{solid.nu})$	Pa	Elasticity matrix, 44 component	Domains 1–2

solid.D45	0	Pa	Elasticity matrix, 45 component	Domains 1–2
solid.D46	0	Pa	Elasticity matrix, 46 component	Domains 1–2
solid.D55	$0.5 * \text{solid.E} / (1 + \text{solid.nu})$	Pa	Elasticity matrix, 55 component	Domains 1–2
solid.D56	0	Pa	Elasticity matrix, 56 component	Domains 1–2
solid.D66	$0.5 * \text{solid.E} / (1 + \text{solid.nu})$	Pa	Elasticity matrix, 66 component	Domains 1–2
solid.K	$\text{solid.E} / (3 * (1 - 2 * \text{solid.nu}))$	N/m ²	Bulk modulus	Domains 1–2
solid.Eequ	solid.E	Pa	Equivalent Young's modulus	Domains 1–2
solid.nuequ	solid.nu	1	Equivalent Poisson's ratio	Domains 1–2
solid.Gequ	solid.G	N/m ²	Equivalent shear modulus	Domains 1–2
solid.cp	$\text{sqrt}((\text{solid.K} + 4 * \text{solid.G} / 3) / \text{solid.rho})$	m/s	Pressure-wave speed	Domains 1–2
solid.cs	$\text{sqrt}(\text{solid.G} / \text{solid.rho})$	m/s	Shear-wave speed	Domains 1–2
solid.E	material.E	Pa	Young's modulus	Domains 1–2
solid.nu	material.nu	1	Poisson's ratio	Domains 1–2
solid.G	$0.5 * \text{solid.E} / (1 + \text{solid.nu})$	N/m ²	Shear modulus	Domains 1–2
solid.lamLame	$\text{solid.E} * \text{solid.nu} / ((1 + \text{solid.nu}) * (1 - 2 * \text{solid.nu}))$	N/m ²	Lamé parameter λ	Domains 1–2
solid.muLame	$0.5 * \text{solid.E} / (1 + \text{solid.nu})$	N/m ²	Lamé parameter μ	Domains 1–2
solid.Cgl11	solid.D11+solid.D12+solid.D13	Pa	C:g tensor, local coordinate system, 11 component	Domains 1–2
solid.Cgl12	solid.D14+solid.D24+solid.D34	Pa	C:g tensor, local coordinate system, 12 component	Domains 1–2
solid.Cgl13	solid.D16+solid.D26+solid.D36	Pa	C:g tensor, local coordinate system, 13 component	Domains 1–2
solid.Cgl22	solid.D12+solid.D22+solid.D23	Pa	C:g tensor, local coordinate system, 22 component	Domains 1–2
solid.Cgl23	solid.D15+solid.D25+solid.D35	Pa	C:g tensor, local coordinate system, 23 component	Domains 1–2

solid.Cgl33	solid.D13+solid.D23+solid.D33	Pa	C:g tensor, local coordinate system, 33 component	Domains 1–2
solid.eXX	uX	1	Strain tensor, XX component	Domains 1–2
solid.eXY	0.5*(uY+vX)	1	Strain tensor, XY component	Domains 1–2
solid.eXZ	0	1	Strain tensor, XZ component	Domains 1–2
solid.eYY	vY	1	Strain tensor, YY component	Domains 1–2
solid.eYZ	0	1	Strain tensor, YZ component	Domains 1–2
solid.eZZ	0	1	Strain tensor, ZZ component	Domains 1–2
solid.el11	solid.eXX	1	Strain tensor, local coordinate system, 11 component	Domains 1–2
solid.el12	solid.eXY	1	Strain tensor, local coordinate system, 12 component	Domains 1–2
solid.el13	solid.eXZ	1	Strain tensor, local coordinate system, 13 component	Domains 1–2
solid.el22	solid.eYY	1	Strain tensor, local coordinate system, 22 component	Domains 1–2
solid.el23	solid.eYZ	1	Strain tensor, local coordinate system, 23 component	Domains 1–2
solid.el33	solid.eZZ	1	Strain tensor, local coordinate system, 33 component	Domains 1–2
solid.eel11	solid.el11-solid.eil11-solid.eiel11	1	Elastic strain tensor, local coordinate system, 11 component	Domains 1–2
solid.eel12	solid.el12-solid.eil12-solid.eiel12	1	Elastic strain tensor, local coordinate	Domains 1–2

			system, 12 component	
solid.eel13	solid.el13-solid.eil13-solid.eiel13	1	Elastic strain tensor, local coordinate system, 13 component	Domains 1–2
solid.eel22	solid.el22-solid.eil22-solid.eiel22	1	Elastic strain tensor, local coordinate system, 22 component	Domains 1–2
solid.eel23	solid.el23-solid.eil23-solid.eiel23	1	Elastic strain tensor, local coordinate system, 23 component	Domains 1–2
solid.eel33	solid.el33-solid.eil33-solid.eiel33	1	Elastic strain tensor, local coordinate system, 33 component	Domains 1–2
solid.Cel11	1+2*solid.eel11	1	Elastic Cauchy-Green tensor, local coordinate system, 11 component	Domains 1–2
solid.Cel12	2*solid.eel12	1	Elastic Cauchy-Green tensor, local coordinate system, 12 component	Domains 1–2
solid.Cel13	2*solid.eel13	1	Elastic Cauchy-Green tensor, local coordinate system, 13 component	Domains 1–2
solid.Cel22	1+2*solid.eel22	1	Elastic Cauchy-Green tensor, local coordinate system, 22 component	Domains 1–2
solid.Cel23	2*solid.eel23	1	Elastic Cauchy-Green tensor, local coordinate system, 23 component	Domains 1–2

solid.Cel33	1+2*solid.eel33	1	Elastic Cauchy-Green tensor, local coordinate system, 33 component	Domains 1–2
solid.eil11	0	1	Initial strain tensor, local coordinate system, 11 component	Domains 1–2
solid.eil12	0	1	Initial strain tensor, local coordinate system, 12 component	Domains 1–2
solid.eil13	0	1	Initial strain tensor, local coordinate system, 13 component	Domains 1–2
solid.eil22	0	1	Initial strain tensor, local coordinate system, 22 component	Domains 1–2
solid.eil23	0	1	Initial strain tensor, local coordinate system, 23 component	Domains 1–2
solid.eil33	0	1	Initial strain tensor, local coordinate system, 33 component	Domains 1–2
solid.eiel11	0	1	Inelastic strain tensor, local coordinate system, 11 component	Domains 1–2
solid.eiel12	0	1	Inelastic strain tensor, local coordinate system, 12 component	Domains 1–2
solid.eiel13	0	1	Inelastic strain tensor, local coordinate	Domains 1–2

			system, 13 component	
solid.eiel22	0	1	Inelastic strain tensor, local coordinate system, 22 component	Domains 1–2
solid.eiel23	0	1	Inelastic strain tensor, local coordinate system, 23 component	Domains 1–2
solid.eiel33	0	1	Inelastic strain tensor, local coordinate system, 33 component	Domains 1–2
solid.evol	solid.eXX+solid.eYY+solid.eZZ	1	Volumetric strain	Domains 1–2
solid.J	solid.FdxX*solid.FdyY*solid.FdzZ+solid.FdxY*solid.FdyZ*solid.FdzX+solid.FdxZ*solid.FdyX*solid.FdzY-solid.FdxX*solid.FdyZ*solid.FdzY-solid.FdxY*solid.FdyX*solid.FdzZ-solid.FdxZ*solid.FdyY*solid.FdzX	1	Volume ratio	Domains 1–2
solid.Ceil11	(solid.Cel22*solid.Cel33-solid.Cel23^2)/(solid.Cel11*solid.Cel22*solid.Cel33+2*solid.Cel12*solid.Cel23*solid.Cel13-solid.Cel11*solid.Cel23^2-solid.Cel12^2*solid.Cel33-solid.Cel22*solid.Cel13^2)	1	Elastic Cauchy-Green tensor inverse, local coordinate system, 11 component	Domains 1–2
solid.Ceil12	(solid.Cel23*solid.Cel13-solid.Cel12*solid.Cel33)/(solid.Cel11*solid.Cel22*solid.Cel33+2*solid.Cel12*solid.Cel23*solid.Cel13-solid.Cel11*solid.Cel23^2-solid.Cel12^2*solid.Cel33-solid.Cel22*solid.Cel13^2)	1	Elastic Cauchy-Green tensor inverse, local coordinate system, 12 component	Domains 1–2
solid.Ceil13	(solid.Cel12*solid.Cel23-solid.Cel22*solid.Cel13)/(solid.Cel11*solid.Cel22*solid.Cel13)	1	Elastic Cauchy-Green tensor inverse, local	Domains 1–2

	d.Cel33+2*solid.Cel12*solid.Cel23*solid.Cel13-solid.Cel11*solid.Cel23^2-solid.Cel12^2*solid.Cel33-solid.Cel22*solid.Cel13^2)		coordinate system, 13 component	
solid.Ceil22	(solid.Cel11*solid.Cel33-solid.Cel13^2)/(solid.Cel11*solid.Cel22*solid.Cel33+2*solid.Cel12*solid.Cel23*solid.Cel13-solid.Cel11*solid.Cel23^2-solid.Cel12^2*solid.Cel33-solid.Cel22*solid.Cel13^2)	1	Elastic Cauchy-Green tensor inverse, local coordinate system, 22 component	Domains 1–2
solid.Ceil23	(solid.Cel12*solid.Cel13-solid.Cel11*solid.Cel23)/(solid.Cel11*solid.Cel22*solid.Cel33+2*solid.Cel12*solid.Cel23*solid.Cel13-solid.Cel11*solid.Cel23^2-solid.Cel12^2*solid.Cel33-solid.Cel22*solid.Cel13^2)	1	Elastic Cauchy-Green tensor inverse, local coordinate system, 23 component	Domains 1–2
solid.Ceil33	(solid.Cel11*solid.Cel22-solid.Cel12^2)/(solid.Cel11*solid.Cel22*solid.Cel33+2*solid.Cel12*solid.Cel23*solid.Cel13-solid.Cel11*solid.Cel23^2-solid.Cel12^2*solid.Cel33-solid.Cel22*solid.Cel13^2)	1	Elastic Cauchy-Green tensor inverse, local coordinate system, 33 component	Domains 1–2
solid.Jel	sqrt(solid.Cel11*solid.Cel22*solid.Cel33+2*solid.Cel12*solid.Cel23*solid.Cel13-solid.Cel11*solid.Cel23^2-solid.Cel12^2*solid.Cel33-solid.Cel22*solid.Cel13^2)	1	Elastic volume ratio	Domains 1–2
solid.eX	solid.eXX	1	Strain tensor, X component	Domains 1–2
solid.eY	solid.eYY	1	Strain tensor, Y component	Domains 1–2
solid.eZ	solid.eZZ	1	Strain tensor, Z component	Domains 1–2
solid.Sil11	0	N/m ²	Initial stress tensor, local coordinate system, 11 component	Domains 1–2
solid.Sil12	0	N/m ²	Initial stress tensor, local	Domains 1–2

			coordinate system, 12 component	
solid.Sil13	0	N/m ²	Initial stress tensor, local coordinate system, 13 component	Domains 1–2
solid.Sil22	0	N/m ²	Initial stress tensor, local coordinate system, 22 component	Domains 1–2
solid.Sil23	0	N/m ²	Initial stress tensor, local coordinate system, 23 component	Domains 1–2
solid.Sil33	0	N/m ²	Initial stress tensor, local coordinate system, 33 component	Domains 1–2
solid.Fiil11	1	1	Inelastic deformation gradient inverse, local coordinate system, 11 component	Domains 1–2
solid.Fiil21	0	1	Inelastic deformation gradient inverse, local coordinate system, 21 component	Domains 1–2
solid.Fiil31	0	1	Inelastic deformation gradient inverse, local coordinate system, 31 component	Domains 1–2
solid.Fiil12	0	1	Inelastic deformation gradient inverse, local coordinate system, 12 component	Domains 1–2

solid.Fiil22	1	1	Inelastic deformation gradient inverse, local coordinate system, 22 component	Domains 1–2
solid.Fiil32	0	1	Inelastic deformation gradient inverse, local coordinate system, 32 component	Domains 1–2
solid.Fiil13	0	1	Inelastic deformation gradient inverse, local coordinate system, 13 component	Domains 1–2
solid.Fiil23	0	1	Inelastic deformation gradient inverse, local coordinate system, 23 component	Domains 1–2
solid.Fiil33	1	1	Inelastic deformation gradient inverse, local coordinate system, 33 component	Domains 1–2
solid.Sl11	solid.Sil11+(solid.Fiil11*(solid.D11*solid.eel11+solid.D12*solid.eel22+solid.D13*solid.eel33+2*solid.D14*solid.eel12+2*solid.D15*solid.eel23+2*solid.D16*solid.eel13)+solid.Fiil12*(solid.D14*solid.eel11+solid.D24*solid.eel22+solid.D34*solid.eel33+2*solid.D44*solid.eel12+2*solid.D45*solid.eel23+2*solid.D46*solid.eel13)+solid.Fiil13*(solid.D16*solid.eel11+solid.D26*solid.eel22+solid.D36*solid.eel33+2*solid.D46*solid.eel12+2*solid.D56*solid.eel23+2*solid.D66*solid.eel13))*solid.Fiil	N/m ²	Second Piola-Kirchhoff stress, local coordinate system, 11 component	Domains 1–2

	$11 + (\text{solid.Fiil11} * (\text{solid.D14} * \text{solid.eel11} + \text{solid.D24} * \text{solid.eel22} + \text{solid.D34} * \text{solid.eel33} + 2 * \text{solid.D44} * \text{solid.eel12} + 2 * \text{solid.D45} * \text{solid.eel23} + 2 * \text{solid.D46} * \text{solid.eel13})) + \text{solid.Fiil12} * (\text{solid.D12} * \text{solid.eel11} + \text{solid.D22} * \text{solid.eel22} + \text{solid.D23} * \text{solid.eel33} + 2 * \text{solid.D24} * \text{solid.eel12} + 2 * \text{solid.D25} * \text{solid.eel23} + 2 * \text{solid.D26} * \text{solid.eel13}) + \text{solid.Fiil13} * (\text{solid.D15} * \text{solid.eel11} + \text{solid.D25} * \text{solid.eel22} + \text{solid.D35} * \text{solid.eel33} + 2 * \text{solid.D45} * \text{solid.eel12} + 2 * \text{solid.D55} * \text{solid.eel23} + 2 * \text{solid.D56} * \text{solid.eel13})) * \text{solid.Fiil12} + (\text{solid.Fiil11} * (\text{solid.D16} * \text{solid.eel11} + \text{solid.D26} * \text{solid.eel22} + \text{solid.D36} * \text{solid.eel33} + 2 * \text{solid.D46} * \text{solid.eel12} + 2 * \text{solid.D56} * \text{solid.eel23} + 2 * \text{solid.D66} * \text{solid.eel13})) + \text{solid.Fiil12} * (\text{solid.D15} * \text{solid.eel11} + \text{solid.D25} * \text{solid.eel22} + \text{solid.D35} * \text{solid.eel33} + 2 * \text{solid.D45} * \text{solid.eel12} + 2 * \text{solid.D55} * \text{solid.eel23} + 2 * \text{solid.D56} * \text{solid.eel13}) + \text{solid.Fiil13} * (\text{solid.D13} * \text{solid.eel11} + \text{solid.D23} * \text{solid.eel22} + \text{solid.D33} * \text{solid.eel33} + 2 * \text{solid.D34} * \text{solid.eel12} + 2 * \text{solid.D35} * \text{solid.eel23} + 2 * \text{solid.D36} * \text{solid.eel13})) * \text{solid.Fiil13}$			
solid.SI12	$\text{solid.Sil12} + (\text{solid.Fiil11} * (\text{solid.D11} * \text{solid.eel11} + \text{solid.D12} * \text{solid.eel22} + \text{solid.D13} * \text{solid.eel33} + 2 * \text{solid.D14} * \text{solid.eel12} + 2 * \text{solid.D15} * \text{solid.eel23} + 2 * \text{solid.D16} * \text{solid.eel13})) + \text{solid.Fiil12} * (\text{solid.D14} * \text{solid.eel11} + \text{solid.D24} * \text{solid.eel22} + \text{solid.D34} * \text{solid.eel33} + 2 * \text{solid.D44} * \text{solid.eel12} + 2 * \text{solid.D45} * \text{solid.eel23} + 2 * \text{solid.D46} * \text{solid.eel13}) + \text{solid.Fiil13} * (\text{solid.D13} * \text{solid.eel11} + \text{solid.D23} * \text{solid.eel22} + \text{solid.D33} * \text{solid.eel33} + 2 * \text{solid.D34} * \text{solid.eel12} + 2 * \text{solid.D35} * \text{solid.eel23} + 2 * \text{solid.D36} * \text{solid.eel13})) * \text{solid.Fiil13}$	N/m ²	Second Piola-Kirchhoff stress, local coordinate system, 12 component	Domains 1–2

	$\begin{aligned} & \text{id.Fiil13} * (\text{solid.D16} * \text{solid.eel11} + \text{solid.D26} * \text{solid.eel22} \\ & + \text{solid.D36} * \text{solid.eel33} + 2 * \text{solid.D46} * \text{solid.eel12} + 2 * \text{solid.D56} * \text{solid.eel23} + 2 * \text{solid.D66} * \text{solid.eel13}) * \text{solid.Fiil21} \\ & + (\text{solid.Fiil11} * (\text{solid.D14} * \text{solid.eel11} + \text{solid.D24} * \text{solid.eel22} + \text{solid.D34} * \text{solid.eel33} + 2 * \text{solid.D44} * \text{solid.eel12} + 2 * \text{solid.D45} * \text{solid.eel23} + 2 * \text{solid.D46} * \text{solid.eel13}) + \text{solid.Fiil12} * (\text{solid.D12} * \text{solid.eel11} + \text{solid.D22} * \text{solid.eel22} + \text{solid.D23} * \text{solid.eel33} + 2 * \text{solid.D24} * \text{solid.eel12} + 2 * \text{solid.D25} * \text{solid.eel23} + 2 * \text{solid.D26} * \text{solid.eel13}) + \text{solid.Fiil13} * (\text{solid.D15} * \text{solid.eel11} + \text{solid.D25} * \text{solid.eel22} + \text{solid.D35} * \text{solid.eel33} + 2 * \text{solid.D45} * \text{solid.eel12} + 2 * \text{solid.D55} * \text{solid.eel23} + 2 * \text{solid.D56} * \text{solid.eel13})) * \text{solid.Fiil22} \\ & + (\text{solid.Fiil11} * (\text{solid.D16} * \text{solid.eel11} + \text{solid.D26} * \text{solid.eel22} + \text{solid.D36} * \text{solid.eel33} + 2 * \text{solid.D46} * \text{solid.eel12} + 2 * \text{solid.D56} * \text{solid.eel23} + 2 * \text{solid.D66} * \text{solid.eel13}) + \text{solid.Fiil12} * (\text{solid.D15} * \text{solid.eel11} + \text{solid.D25} * \text{solid.eel22} + \text{solid.D35} * \text{solid.eel33} + 2 * \text{solid.D45} * \text{solid.eel12} + 2 * \text{solid.D55} * \text{solid.eel23} + 2 * \text{solid.D56} * \text{solid.eel13}) + \text{solid.Fiil13} * (\text{solid.D13} * \text{solid.eel11} + \text{solid.D23} * \text{solid.eel22} + \text{solid.D33} * \text{solid.eel33} + 2 * \text{solid.D34} * \text{solid.eel12} + 2 * \text{solid.D35} * \text{solid.eel23} + 2 * \text{solid.D36} * \text{solid.eel13})) * \text{solid.Fiil23} \end{aligned}$			
solid.Sl13	$\text{solid.Sil13} + (\text{solid.Fiil11} * (\text{solid.D11} * \text{solid.eel11} + \text{solid.D12} * \text{solid.eel22} + \text{solid.D13} * \text{solid.eel33} + 2 * \text{solid.D14} * \text{solid.eel12} + 2 * \text{solid.D15} * \text{solid.eel23} + 2 * \text{solid.D16} * \text{solid.eel13})) * \text{solid.Fiil23}$	N/m ²	Second Piola-Kirchhoff stress, local coordinate system, 13 component	Domains 1–2

	<p>l13)+solid.Fiil12*(solid.D14 *solid.eel11+solid.D24*soli d.eel22+solid.D34*solid.eel 33+2*solid.D44*solid.eel12 +2*solid.D45*solid.eel23+2 *solid.D46*solid.eel13)+sol id.Fiil13*(solid.D16*solid.e el11+solid.D26*solid.eel22 +solid.D36*solid.eel33+2*s olid.D46*solid.eel12+2*soli d.D56*solid.eel23+2*solid. D66*solid.eel13))*solid.Fiil 31+(solid.Fiil11*(solid.D14* solid.eel11+solid.D24*solid .eel22+solid.D34*solid.eel3 3+2*solid.D44*solid.eel12+ 2*solid.D45*solid.eel23+2* solid.D46*solid.eel13)+soli d.Fiil12*(solid.D12*solid.ee l11+solid.D22*solid.eel22+ solid.D23*solid.eel33+2*so lid.D24*solid.eel12+2*solid .D25*solid.eel23+2*solid.D 26*solid.eel13)+solid.Fiil13 *(solid.D15*solid.eel11+sol id.D25*solid.eel22+solid.D 35*solid.eel33+2*solid.D45 *solid.eel12+2*solid.D55*s olid.eel23+2*solid.D56*soli d.eel13))*solid.Fiil32+(solid .Fiil11*(solid.D16*solid.eel 11+solid.D26*solid.eel22+s olid.D36*solid.eel33+2*soli d.D46*solid.eel12+2*solid. D56*solid.eel23+2*solid.D 66*solid.eel13)+solid.Fiil12 *(solid.D15*solid.eel11+sol id.D25*solid.eel22+solid.D 35*solid.eel33+2*solid.D45 *solid.eel12+2*solid.D55*s olid.eel23+2*solid.D56*soli d.eel13)+solid.Fiil13*(solid. D13*solid.eel11+solid.D23 *solid.eel22+solid.D33*soli d.eel33+2*solid.D34*solid. eel12+2*solid.D35*solid.ee l23+2*solid.D36*solid.eel1 3))*solid.Fiil33</p>			

solid.SI22	<p>solid.SI22+(solid.Fiil21*(solid.D11*solid.eel11+solid.D12*solid.eel22+solid.D13*solid.eel33+2*solid.D14*solid.eel12+2*solid.D15*solid.eel23+2*solid.D16*solid.eel13)+solid.Fiil22*(solid.D14*solid.eel11+solid.D24*solid.eel22+solid.D34*solid.eel33+2*solid.D44*solid.eel12+2*solid.D45*solid.eel23+2*solid.D46*solid.eel13)+solid.Fiil23*(solid.D16*solid.eel11+solid.D26*solid.eel22+solid.D36*solid.eel33+2*solid.D46*solid.eel12+2*solid.D56*solid.eel23+2*solid.D66*solid.eel13))*solid.Fiil21+(solid.Fiil21*(solid.D14*solid.eel11+solid.D24*solid.eel22+solid.D34*solid.eel33+2*solid.D44*solid.eel12+2*solid.D45*solid.eel23+2*solid.D46*solid.eel13)+solid.Fiil22*(solid.D12*solid.eel11+solid.D22*solid.eel22+solid.D23*solid.eel33+2*solid.D24*solid.eel12+2*solid.D25*solid.eel23+2*solid.D26*solid.eel13)+solid.Fiil23*(solid.D15*solid.eel11+solid.D25*solid.eel22+solid.D35*solid.eel33+2*solid.D45*solid.eel12+2*solid.D55*solid.eel23+2*solid.D56*solid.eel13))*solid.Fiil22+(solid.Fiil21*(solid.D16*solid.eel11+solid.D26*solid.eel22+solid.D36*solid.eel33+2*solid.D46*solid.eel12+2*solid.D56*solid.eel23+2*solid.D66*solid.eel13)+solid.Fiil22*(solid.D15*solid.eel11+solid.D25*solid.eel22+solid.D35*solid.eel33+2*solid.D45*solid.eel12+2*solid.D55*solid.eel23+2*solid.D56*solid.eel13)+solid.Fiil23*(solid.</p>	N/m ²	Second Piola-Kirchhoff stress, local coordinate system, 22 component	Domains 1–2
------------	---	------------------	--	-------------

	D13*solid.eel11+solid.D23 *solid.eel22+solid.D33*soli d.eel33+2*solid.D34*solid. eel12+2*solid.D35*solid.ee l23+2*solid.D36*solid.eel1 3))*solid.Fiil23			
solid.SI23	solid.Sil23+(solid.Fiil21*(sol id.D11*solid.eel11+solid.D 12*solid.eel22+solid.D13*s olid.eel33+2*solid.D14*soli d.eel12+2*solid.D15*solid. eel23+2*solid.D16*solid.ee l13)+solid.Fiil22*(solid.D14 *solid.eel11+solid.D24*soli d.eel22+solid.D34*solid.eel 33+2*solid.D44*solid.eel12 +2*solid.D45*solid.eel23+2 *solid.D46*solid.eel13)+sol id.Fiil23*(solid.D16*solid.e el11+solid.D26*solid.eel22 +solid.D36*solid.eel33+2*s olid.D46*solid.eel12+2*soli d.D56*solid.eel23+2*solid. D66*solid.eel13))*solid.Fiil 31+(solid.Fiil21*(solid.D14* solid.eel11+solid.D24*solid .eel22+solid.D34*solid.eel3 3+2*solid.D44*solid.eel12+ 2*solid.D45*solid.eel23+2* solid.D46*solid.eel13)+soli d.Fiil22*(solid.D12*solid.ee l11+solid.D22*solid.eel22+ solid.D23*solid.eel33+2*so lid.D24*solid.eel12+2*solid .D25*solid.eel23+2*solid.D 26*solid.eel13)+solid.Fiil23 *(solid.D15*solid.eel11+sol id.D25*solid.eel22+solid.D 35*solid.eel33+2*solid.D45 *solid.eel12+2*solid.D55*s olid.eel23+2*solid.D56*soli d.eel13))*solid.Fiil32+(solid .Fiil21*(solid.D16*solid.eel 11+solid.D26*solid.eel22+s olid.D36*solid.eel33+2*soli d.D46*solid.eel12+2*solid. D56*solid.eel23+2*solid.D 66*solid.eel13)+solid.Fiil22	N/m ²	Second Piola- Kirchhoff stress, local coordinate system, 23 component	Domains 1–2

	<p>*(solid.D15*solid.eel11+solid.D25*solid.eel22+solid.D35*solid.eel33+2*solid.D45*solid.eel12+2*solid.D55*solid.eel23+2*solid.D56*solid.eel13)+solid.Fiil23*(solid.D13*solid.eel11+solid.D23*solid.eel22+solid.D33*solid.eel33+2*solid.D34*solid.eel12+2*solid.D35*solid.eel23+2*solid.D36*solid.eel13))*solid.Fiil33</p>			
solid.SI33	<p>solid.Sil33+(solid.Fiil31*(solid.D11*solid.eel11+solid.D12*solid.eel22+solid.D13*solid.eel33+2*solid.D14*solid.eel12+2*solid.D15*solid.eel23+2*solid.D16*solid.eel13)+solid.Fiil32*(solid.D14*solid.eel11+solid.D24*solid.eel22+solid.D34*solid.eel33+2*solid.D44*solid.eel12+2*solid.D45*solid.eel23+2*solid.D46*solid.eel13)+solid.Fiil33*(solid.D16*solid.eel11+solid.D26*solid.eel22+solid.D36*solid.eel33+2*solid.D46*solid.eel12+2*solid.D56*solid.eel23+2*solid.D66*solid.eel13))*solid.Fiil31+(solid.Fiil31*(solid.D14*solid.eel11+solid.D24*solid.eel22+solid.D34*solid.eel33+2*solid.D44*solid.eel12+2*solid.D45*solid.eel23+2*solid.D46*solid.eel13)+solid.Fiil32*(solid.D12*solid.eel11+solid.D22*solid.eel22+solid.D23*solid.eel33+2*solid.D24*solid.eel12+2*solid.D25*solid.eel23+2*solid.D26*solid.eel13)+solid.Fiil33*(solid.D15*solid.eel11+solid.D25*solid.eel22+solid.D35*solid.eel33+2*solid.D45*solid.eel12+2*solid.D55*solid.eel23+2*solid.D56*solid.eel13))*solid.Fiil32+(solid</p>	N/m ²	Second Piola-Kirchhoff stress, local coordinate system, 33 component	Domains 1–2

	.Fiil31*(solid.D16*solid.eel11+solid.D26*solid.eel22+solid.D36*solid.eel33+2*solid.D46*solid.eel12+2*solid.D56*solid.eel23+2*solid.D66*solid.eel13)+solid.Fiil32*(solid.D15*solid.eel11+solid.D25*solid.eel22+solid.D35*solid.eel33+2*solid.D45*solid.eel12+2*solid.D55*solid.eel23+2*solid.D56*solid.eel13)+solid.Fiil33*(solid.D13*solid.eel11+solid.D23*solid.eel22+solid.D33*solid.eel33+2*solid.D34*solid.eel12+2*solid.D35*solid.eel23+2*solid.D36*solid.eel13))*solid.Fiil33			
solid.SXX	solid.SI11	N/m ²	Second Piola-Kirchhoff stress, XX component	Domains 1–2
solid.SXY	solid.SI12	N/m ²	Second Piola-Kirchhoff stress, XY component	Domains 1–2
solid.SXZ	solid.SI13	N/m ²	Second Piola-Kirchhoff stress, XZ component	Domains 1–2
solid.SYY	solid.SI22	N/m ²	Second Piola-Kirchhoff stress, YY component	Domains 1–2
solid.SYZ	solid.SI23	N/m ²	Second Piola-Kirchhoff stress, YZ component	Domains 1–2
solid.SZZ	solid.SI33	N/m ²	Second Piola-Kirchhoff stress, ZZ component	Domains 1–2
solid.u_ttX	d(uTIME,TIME)	m/s ²	Acceleration, X component	Domains 1–2
solid.u_ttY	d(vTIME,TIME)	m/s ²	Acceleration, Y component	Domains 1–2
solid.u_ttZ	0	m/s ²	Acceleration, Z component	Domains 1–2
solid.u_tX	uTIME	m/s	Velocity, X component	Domains 1–2
solid.u_tY	vTIME	m/s	Velocity, Y component	Domains 1–2
solid.u_tZ	0	m/s	Velocity, Z component	Domains 1–2

solid.accX	solid.u_ttX	m/s ²	Total acceleration, X component	Domains 1–2
solid.accY	solid.u_ttY	m/s ²	Total acceleration, Y component	Domains 1–2
solid.accZ	solid.u_ttZ	m/s ²	Total acceleration, Z component	Domains 1–2
solid.vel	$\sqrt{\text{real}(\text{solid.u_tX})^2 + \text{real}(\text{solid.u_tY})^2 + \text{real}(\text{solid.u_tZ})^2}$	m/s	Velocity magnitude	Domains 1–2
solid.acc	$\sqrt{\text{real}(\text{solid.accX})^2 + \text{real}(\text{solid.accY})^2 + \text{real}(\text{solid.accZ})^2}$	m/s ²	Acceleration magnitude	Domains 1–2
solid.G0	solid.Gequ	N/m ²	Instantaneous shear modulus	Domains 1–2
solid.Ldx	d(solid.gradUxX,TIME)	1/s	Rate of strain tensor, x component	Domains 1–2
solid.Ldxy	0.5*(d(solid.gradUxY,TIME) + d(solid.gradUyX,TIME))	1/s	Rate of strain tensor, xy component	Domains 1–2
solid.Ldxz	0.5*(d(solid.gradUxZ,TIME) + d(solid.gradUzX,TIME))	1/s	Rate of strain tensor, xz component	Domains 1–2
solid.Ldy	d(solid.gradUyY,TIME)	1/s	Rate of strain tensor, y component	Domains 1–2
solid.Ldyz	0.5*(d(solid.gradUyZ,TIME) + d(solid.gradUzY,TIME))	1/s	Rate of strain tensor, yz component	Domains 1–2
solid.Ldz	d(solid.gradUzZ,TIME)	1/s	Rate of strain tensor, z component	Domains 1–2
solid.Lwx	0	1/s	Spin tensor, x component	Domains 1–2
solid.Lwxy	0.5*(d(solid.gradUxY,TIME) - d(solid.gradUyX,TIME))	1/s	Spin tensor, xy component	Domains 1–2
solid.Lwxz	0.5*(d(solid.gradUxZ,TIME) - d(solid.gradUzX,TIME))	1/s	Spin tensor, xz component	Domains 1–2
solid.Lwy	0	1/s	Spin tensor, y component	Domains 1–2
solid.Lwyz	0.5*(d(solid.gradUyZ,TIME) - d(solid.gradUzY,TIME))	1/s	Spin tensor, yz component	Domains 1–2
solid.Lwz	0	1/s	Spin tensor, z component	Domains 1–2

solid.Ws	$0.5*((\text{solid.SI11}+\text{solid.Sil11}) * \text{solid.eel11}+2*(\text{solid.SI12}+\text{solid.Sil12})*\text{solid.eel12}+2*(\text{solid.SI13}+\text{solid.Sil13})*\text{solid.eel13}+(\text{solid.SI22}+\text{solid.Sil22})*\text{solid.eel22}+2*(\text{solid.SI23}+\text{solid.Sil23})*\text{solid.eel23}+(\text{solid.SI33}+\text{solid.Sil33})*\text{solid.eel33})$	J/m^3	Elastic strain energy density	Domains 1–2
solid.Wh	solid.Ws	J/m^3	Stored energy density	Domains 1–2
solid.Ws_tot	root.comp1.solid.lemm1.int1(solid.Ws*solid.d)	J	Total elastic strain energy	Global
solid.Wh_tot	root.comp1.solid.lemm1.int2(solid.Ws*solid.d)	J	Total stored energy	Global
solid.disp	$\text{sqrt}(\text{real}(u)^2+\text{real}(v)^2)$	m	Total displacement	Domains 1–2
solid.PxX	$\text{solid.FdxX}*\text{solid.SX}+\text{solid.FdxY}*\text{solid.SXY}+\text{solid.FdxZ}*\text{solid.SXZ}$	N/m^2	First Piola-Kirchhoff stress, xX component	Domains 1–2
solid.PyX	$\text{solid.FdyX}*\text{solid.SX}+\text{solid.FdyY}*\text{solid.SXY}+\text{solid.FdyZ}*\text{solid.SXZ}$	N/m^2	First Piola-Kirchhoff stress, yX component	Domains 1–2
solid.PzX	$\text{solid.FdzX}*\text{solid.SX}+\text{solid.FdzY}*\text{solid.SXY}+\text{solid.FdzZ}*\text{solid.SXZ}$	N/m^2	First Piola-Kirchhoff stress, zX component	Domains 1–2
solid.PxY	$\text{solid.FdxX}*\text{solid.SXY}+\text{solid.FdxY}*\text{solid.SY}+\text{solid.FdxZ}*\text{solid.SYZ}$	N/m^2	First Piola-Kirchhoff stress, xY component	Domains 1–2
solid.PyY	$\text{solid.FdyX}*\text{solid.SXY}+\text{solid.FdyY}*\text{solid.SY}+\text{solid.FdyZ}*\text{solid.SYZ}$	N/m^2	First Piola-Kirchhoff stress, yY component	Domains 1–2
solid.PzY	$\text{solid.FdzX}*\text{solid.SXY}+\text{solid.FdzY}*\text{solid.SY}+\text{solid.FdzZ}*\text{solid.SYZ}$	N/m^2	First Piola-Kirchhoff stress, zY component	Domains 1–2
solid.PxZ	$\text{solid.FdxX}*\text{solid.SXZ}+\text{solid.FdxY}*\text{solid.SYZ}+\text{solid.FdxZ}*\text{solid.SZ}$	N/m^2	First Piola-Kirchhoff stress, xZ component	Domains 1–2
solid.PyZ	$\text{solid.FdyX}*\text{solid.SXZ}+\text{solid.FdyY}*\text{solid.SYZ}+\text{solid.FdyZ}*\text{solid.SZ}$	N/m^2	First Piola-Kirchhoff stress, yZ component	Domains 1–2
solid.PzZ	$\text{solid.FdzX}*\text{solid.SXZ}+\text{solid.FdzY}*\text{solid.SYZ}+\text{solid.FdzZ}*\text{solid.SZ}$	N/m^2	First Piola-Kirchhoff stress, zZ component	Domains 1–2
solid.sx	solid.SX	N/m^2	Stress tensor, x component	Domains 1–2
solid.sxy	solid.SXY	N/m^2	Stress tensor, xy component	Domains 1–2

solid.sxz	solid.SXZ	N/m^2	Stress tensor, xz component	Domains 1–2
solid.sy	solid.SY	N/m^2	Stress tensor, y component	Domains 1–2
solid.syz	solid.SYZ	N/m^2	Stress tensor, yz component	Domains 1–2
solid.sz	solid.SZ	N/m^2	Stress tensor, z component	Domains 1–2
solid.sl11	solid.Sl11	N/m^2	Stress tensor, local coordinate system, 11 component	Domains 1–2
solid.sl12	solid.Sl12	N/m^2	Stress tensor, local coordinate system, 12 component	Domains 1–2
solid.sl13	solid.Sl13	N/m^2	Stress tensor, local coordinate system, 13 component	Domains 1–2
solid.sl22	solid.Sl22	N/m^2	Stress tensor, local coordinate system, 22 component	Domains 1–2
solid.sl23	solid.Sl23	N/m^2	Stress tensor, local coordinate system, 23 component	Domains 1–2
solid.sl33	solid.Sl33	N/m^2	Stress tensor, local coordinate system, 33 component	Domains 1–2
solid.sdevx	solid.sx- (solid.sx+solid.sy+solid.sz)/ 3	N/m^2	Deviatoric stress tensor, x component	Domains 1–2
solid.sdevxy	solid.sxy	N/m^2	Deviatoric stress tensor, xy component	Domains 1–2
solid.sdevxz	solid.sxz	N/m^2	Deviatoric stress tensor, xz component	Domains 1–2
solid.sdevy	solid.sy- (solid.sx+solid.sy+solid.sz)/ 3	N/m^2	Deviatoric stress tensor, y component	Domains 1–2
solid.sdevyz	solid.syz	N/m^2	Deviatoric stress tensor, yz component	Domains 1–2

solid.sdevz	solid.sz- (solid.sx+solid.sy+solid.sz)/ 3	N/m ²	Deviatoric stress tensor, z component	Domains 1–2
solid.SdevX	solid.SX- (solid.SX+solid.SY+solid.SZ) /3	N/m ²	Deviatoric second Piola-Kirchhoff stress, X component	Domains 1–2
solid.SdevXY	solid.SXY	N/m ²	Deviatoric second Piola-Kirchhoff stress, XY component	Domains 1–2
solid.SdevXZ	solid.SXZ	N/m ²	Deviatoric second Piola-Kirchhoff stress, XZ component	Domains 1–2
solid.SdevY	solid.SY- (solid.SX+solid.SY+solid.SZ) /3	N/m ²	Deviatoric second Piola-Kirchhoff stress, Y component	Domains 1–2
solid.SdevYZ	solid.SYZ	N/m ²	Deviatoric second Piola-Kirchhoff stress, YZ component	Domains 1–2
solid.SdevZ	solid.SZ- (solid.SX+solid.SY+solid.SZ) /3	N/m ²	Deviatoric second Piola-Kirchhoff stress, Z component	Domains 1–2
solid.I1s	solid.sl11+solid.sl22+solid.sl33	N/m ²	First principal invariant of stress	Domains 1–2
solid.I2s	0.5*(solid.I1s ² - solid.sl11 ² -2*solid.sl12 ² - 2*solid.sl13 ² -solid.sl22 ² - 2*solid.sl23 ² -solid.sl33 ²)	kg ² /(m ² ·s ⁴)	Second principal invariant of stress	Domains 1–2
solid.I3s	solid.sl11*solid.sl22*solid.sl33+2*solid.sl12*solid.sl23*solid.sl13- solid.sl11*solid.sl23 ² - solid.sl12 ² *solid.sl33- solid.sl22*solid.sl13 ²	kg ³ /(m ³ ·s ⁶)	Third principal invariant of stress	Domains 1–2
solid.II2s	0.5*((solid.sl11- (solid.sl11+solid.sl22+solid.sl33)/3) ² +2*solid.sl12 ² + 2*solid.sl13 ² +(solid.sl22- (solid.sl11+solid.sl22+solid.sl33)/3) ² +2*solid.sl23 ² +(solid.sl33- (solid.sl11+solid.sl22+solid.sl33)/3) ²)	kg ² /(m ² ·s ⁴)	Second invariant of stress deviator	Domains 1–2

solid.II3s	$(\text{solid.sl11} - (\text{solid.sl11} + \text{solid.sl22} + \text{solid.sl33})/3) * (\text{solid.sl22} - (\text{solid.sl11} + \text{solid.sl22} + \text{solid.sl33})/3) * (\text{solid.sl33} - (\text{solid.sl11} + \text{solid.sl22} + \text{solid.sl33})/3) + 2 * \text{solid.sl12} * \text{solid.sl23} * \text{solid.sl13} - (\text{solid.sl11} - (\text{solid.sl11} + \text{solid.sl22} + \text{solid.sl33})/3) * \text{solid.sl23}^2 - \text{solid.sl12}^2 * (\text{solid.sl33} - (\text{solid.sl11} + \text{solid.sl22} + \text{solid.sl33})/3) - (\text{solid.sl22} - (\text{solid.sl11} + \text{solid.sl22} + \text{solid.sl33})/3) * \text{solid.sl13}^2$	$\text{kg}^3/(\text{m}^3 \cdot \text{s}^6)$	Third invariant of stress deviator	Domains 1–2
solid.thetaL	$\text{atan2}(\text{sqrt}(\max(0.14814814814814814 * \text{solid.II2s}^3 - \text{solid.II3s}^2, \text{eps})), \text{solid.II3s}) / 3$	rad	Lode angle	Domains 1–2
solid.eevol	$\text{solid.eel11} + \text{solid.eel22} + \text{solid.eel33}$	1	First invariant of elastic strain tensor	Domains 1–2
solid.eeldev11	$\text{solid.eel11} - (\text{solid.eel11} + \text{solid.eel22} + \text{solid.eel33})/3$	1	Deviatoric elastic strain tensor, local coordinate system, 11 component	Domains 1–2
solid.eeldev12	solid.eel12	1	Deviatoric elastic strain tensor, local coordinate system, 12 component	Domains 1–2
solid.eeldev13	solid.eel13	1	Deviatoric elastic strain tensor, local coordinate system, 13 component	Domains 1–2
solid.eeldev22	$\text{solid.eel22} - (\text{solid.eel11} + \text{solid.eel22} + \text{solid.eel33})/3$	1	Deviatoric elastic strain tensor, local coordinate system, 22 component	Domains 1–2
solid.eeldev23	solid.eel23	1	Deviatoric elastic strain tensor, local coordinate system, 23 component	Domains 1–2

solid.eeldev33	$\text{solid.eel33} - (\text{solid.eel11} + \text{solid.eel22} + \text{solid.eel33})/3$	1	Deviatoric elastic strain tensor, local coordinate system, 33 component	Domains 1–2
solid.II2eel	$0.5 * ((\text{solid.eel11} - (\text{solid.eel11} + \text{solid.eel22} + \text{solid.eel33})/3)^2 + 2 * \text{solid.eel12}^2 + 2 * \text{solid.eel13}^2 + (\text{solid.eel22} - (\text{solid.eel11} + \text{solid.eel22} + \text{solid.eel33})/3)^2 + 2 * \text{solid.eel23}^2 + (\text{solid.eel33} - (\text{solid.eel11} + \text{solid.eel22} + \text{solid.eel33})/3)^2)$	1	Second invariant of deviatoric elastic strain tensor	Domains 1–2
solid.pm	$-(\text{solid.sl11} + \text{solid.sl22} + \text{solid.sl33})/3$	N/m ²	Pressure	Domains 1–2
solid.curlUX	0	1	Curl of displacement, X component	Domains 1–2
solid.curlUY	0	1	Curl of displacement, Y component	Domains 1–2
solid.curlUZ	$\text{solid.gradUyX} - \text{solid.gradUxY}$	1	Curl of displacement, Z component	Domains 1–2
solid.mises	$(3 * \text{solid.II2s})^{0.5}$	N/m ²	von Mises stress	Domains 1–2
solid.tresca	$\text{solid.sp1} - \text{solid.sp3}$	N/m ²	Tresca stress	Domains 1–2
solid.RFx	$\text{react}(u)$	N	Reaction force, x component	Domains 1–2
solid.RFy	$\text{react}(v)$	N	Reaction force, y component	Domains 1–2
solid.RFz	0	N	Reaction force, z component	Domains 1–2
solid.RMx	$\text{solid.RFz} * (y - \text{solid.refpnty}) + \text{solid.RFy} * \text{solid.refpntz}$	N·m	Reaction moment, x component	Domains 1–2
solid.RMy	$-\text{solid.RFz} * (x - \text{solid.refpntx}) - \text{solid.RFx} * \text{solid.refpntz}$	N·m	Reaction moment, y component	Domains 1–2
solid.RMz	$\text{solid.RFy} * (x - \text{solid.refpntx}) - \text{solid.RFx} * (y - \text{solid.refpnty})$	N·m	Reaction moment, z component	Domains 1–2
solid.Tax	$\text{solid.sx} * \text{solid.nx} + \text{solid.sxy} * \text{solid.ny} + \text{solid.sxz} * \text{solid.nz}$	N/m ²	Traction (force/area), x component	Boundaries 1–7

solid.Tay	solid.sxy*solid.nx+solid.sy* solid.ny+solid.syz*solid.nz	N/m ²	Traction (force/area), y component	Boundaries 1– 7
solid.Taz	solid.sxz*solid.nx+solid.syz *solid.ny+solid.sz*solid.nz	N/m ²	Traction (force/area), z component	Boundaries 1– 7

Shape functions

Name	Shape function	Unit	Description	Shape frame	Selection
u	Nodal serendipity (Quadratic)	m	Displacement field, X component	Material	Domains 1–2
v	Nodal serendipity (Quadratic)	m	Displacement field, Y component	Material	Domains 1–2

Weak expressions

Weak expression	Integration order	Integration frame	Selection
(-solid.Sl11*test(solid.el11)- 2*solid.Sl12*test(solid.el12)- 2*solid.Sl13*test(solid.el13)- solid.Sl22*test(solid.el22)- 2*solid.Sl23*test(solid.el23)- solid.Sl33*test(solid.el33))*solid.d	4	Material	Domains 1–2